

Autoantibodies Against β_1 -Adrenoceptor Exaggerated Ventricular Remodeling by Inhibiting CTRP9 Expression

Yunhui Du, PhD;* Shihan Zhang, MD;* Haicun Yu, MD; Ye Wu, MD, PhD; Ning Cao, MD; Wen Wang, MD, PhD; Wenli Xu, PhD; Yuming Li, PhD; Huirong Liu, MD, PhD

Background—Autoantibodies against the second extracellular loop of the β_1 -adrenoceptor (β_1 -AA) act similarly to agonist of β_1 -adrenergic receptor, which plays an important role in the pathophysiological characteristics of ventricular remodeling. Recently, considerable lines of evidence have suggested that CTRP9 (C1q tumor necrosis factor–related protein 9) is a potent cardioprotective cardiokine and protects the heart from ventricular remodeling. The aim of this study was to determine the role of CTRP9 in ventricular remodeling induced by β_1 -AA.

Methods and Results—Blood samples were collected from 131 patients with coronary heart disease and 131 healthy subjects. The serum levels of β_1 -AA and CTRP9 were detected using ELISA. The results revealed that CTRP9 levels in β_1 -AA–positive patients were lower than those in β_1 -AA–negative patients, and serum CTRP9 concentrations were inversely correlated with β_1 -AA. β_1 -AA monoclonal antibodies (β_1 -AAMAbs) were administered in mice with and without rAAV9-cTnT-Full Ctrp9-FLAG virus for 8 weeks. Reverse transcription–polymerase chain reaction/Western analysis showed that cardiomyocyte CTRP9 expression was significantly reduced in β_1 -AAMAb–treated mice. Moreover, compared with the β_1 -AAMAb alone group, cardiac-specific CTRP9 overexpression improved cardiac function, attenuated adverse remodeling, and ameliorated cardiomyocyte apoptosis and fibrosis. Mechanistic studies demonstrated that CTRP9 overexpression decreased the levels of G-protein–coupled receptor kinase 2 and promoted the activation of AMP-dependent kinase pathway. However, cardiac-specific overexpression of CTRP9 had no effect on the levels of cAMP and protein kinase A activity elevated by β_1 -AAMAb.

Conclusions—This study provides the first evidence that the long-term existence of β_1 -AAMAb suppresses cardiac CTRP9 expression and exaggerates cardiac remodeling, suggesting that CTRP9 may be a novel therapeutic target against pathologic remodeling in β_1 -AA–positive patients with coronary heart disease. (*J Am Heart Assoc.* 2019;8:e010475. DOI: 10.1161/JAHA.118.010475.)

Key Words: adrenergic • autoantibody • β_1 • CTRP9 (C1q tumor necrosis factor–related protein 9) • receptor • ventricular remodeling

Ventricular remodeling (VR) plays an important role in the adaptive response to the increased contractility. It is not only a factor associated with heart failure (HF), but also leads to the increased morbidity and mortality of cardiac diseases.¹ Therefore, early inhibition of VR seems to be an effective strategy for delaying the HF in patients with cardiovascular diseases. VR is

a complex process, involving hypertrophy, cardiac fibrosis, and alterations of gene expression and extracellular matrix, which may result in wall thickening.² However, the pathogenic mechanisms underlying VR are not yet well understood.

Autoantibodies against the second extracellular loop of β_1 -adrenoceptors were reported to exist in dilated

From the Beijing Anzhen Hospital, Capital Medical University, Beijing Institute of Heart, Lung and Blood Vessel Diseases, Beijing, China (Y.D.); Department of Physiology and Pathophysiology, School of Basic Medical Sciences (S.Z., H.Y., Y.W., N.C., W.W., W.X., H.L.), and Department of Basic Medical Sciences, Yanjing Medical College (Y.L.), Capital Medical University, Beijing, China; and Zhengzhou Central Hospital affiliated of Zhengzhou University, Henan Province, China (H.Y.).

Accompanying Data S1 and Figures S1 through S5 are available at <https://www.ahajournals.org/doi/suppl/10.1161/JAHA.118.010475>

*Dr Du and Dr Zhang contributed equally to this work.

Correspondence to: Huirong Liu, MD, PhD, Department of Physiology and Pathophysiology, School of Basic Medical Sciences, Capital Medical University, Beijing, China. E-mail: liuhr2000@ccmu.edu.cn or Yuming Li, PhD, Department of Basic Medical Sciences, Yanjing Medical College, Capital Medical University, Beijing, China. E-mail: ymlea@sina.com

Received July 31, 2018; accepted December 17, 2018.

© 2019 The Authors. Published on behalf of the American Heart Association, Inc., by Wiley. This is an open access article under the terms of the Creative Commons Attribution-NonCommercial-NoDerivs License, which permits use and distribution in any medium, provided the original work is properly cited, the use is non-commercial and no modifications or adaptations are made.

Clinical Perspective

What Is New?

- To our knowledge, this study is the first to reveal that autoantibodies against the second extracellular loop of β_1 -adrenergic receptor could decrease the expression of cardioprotective cardiokine CTRP9 (C1q tumor necrosis factor–related protein 9).
- Mechanistic study reveals that CTRP9 ameliorated autoantibodies against the second extracellular loop of β_1 -adrenergic receptor–mediated ventricular remodeling and restored cardiac function via G-protein–coupled receptor kinase 2/adiponectin receptor 1/AMP-dependent kinase signaling pathway.

What Are the Clinical Implications?

- CTRP9 may represent a new therapeutic target for preventing the progression of cardiac remodeling and fibrosis of patients with autoantibodies against the second extracellular loop of β_1 -adrenergic receptor–positive cardiac disease.
- CTRP9 not only plays an important role in myocardial ischemia/reperfusion injury, but also in immune-mediated heart disease.

cardiomyopathy by Wallukat and Wollenberger.³ The level of autoantibodies against the second extracellular loop of β_1 -adrenergic receptor (β_1 -AA) was significantly reduced through the immunoabsorption therapy,⁴ which could lead to an improvement in cardiac function. This finding suggests that the circulating β_1 -AA may be involved in the pathogenesis of cardiovascular diseases. Accumulated evidence indicates that the overstimulation of β -adrenergic receptor (β -AR) may induce adverse myocardial remodeling,^{5–7} and treatment with β_1 -AR–selective antagonist appears to have beneficial effects on cardiac structure and function.⁸ Moreover, several clinical studies have proved that β_1 -AA contribute to dilated cardiomyopathy^{9–13} and HF.^{14,15} Therefore, it is essential to explore the role of β_1 -AA in VR and elucidate its downstream molecular mechanisms.

Cardiokines play an essential role in maintaining normal cardiac functions and respond to VR.^{16,17} CTRP9 (C1q tumor necrosis factor–related protein 9) is a member of the adiponectin paralog CTRP family and highly expressed in the heart, recently identified as a cardiokine modulating cardiac function.¹⁸ CTRP9 improves the prognosis of heart disease via its inhibitory effects on inflammation, post–ischemia–reperfusion injury, and VR.^{19–21} Moreover, CTRP9 was reported as a cell survival molecule, preventing cardiomyocyte death during ischemia–reperfusion injury through adiponectin receptor 1 (AdipoR1)/AMP-dependent kinase (AMPK) or AdipoR1/protein kinase A (PKA) pathways.^{19,21} In addition, CTRP9

attenuated left VR by reducing cardiomyocyte apoptosis and fibrosis.²² However, whether CTRP9 functions as a mediator or inhibitor of VR induced by β_1 -AA is unknown.

Therefore, this study aimed to investigate the role of cardiokine CTRP9 in β_1 -AA–induced VR. In addition, we further explored the mechanisms behind its effects.

Methods

The data, analytic methods, and study materials will be available from the corresponding author on reasonable request to other researchers for purposes of reproducing the results or replicating the procedure.

Subject Recruitment and Sample Preparation

Research ethics committee (Beijing Anzhen Hospital, Capital Medical University, Beijing, China) provided ethical approval, and all recruits provided written and oral informed consents, in accordance with the Declaration of Helsinki. A total of 131 patients with coronary heart disease (CAD) and 131 healthy controls were recruited from Beijing Anzhen Hospital, Capital Medical University. The clinical characteristics of patients with CAD are summarized in Tables 1 and 2. Patients who had at least 1 coronary vessel with >75% luminal stenosis were classified as patients with CAD, as evaluated by a cardiologist. Exclusion criteria included acute congestive HF, cancer, myocardial infarction, chronic renal insufficiency, thyroid disease, and the use of oral corticosteroids. Venous blood samples were collected without anticoagulant. After centrifugation at 4°C, the serum was immediately separated and stored at –80°C until further analysis.

Animals

The animal protocol was approved by the Animal Care and Use Committee of the Capital Medical University. The investigation complied with the National Institutes of Health *Guide for the Care and Use of Laboratory Animals*. All in vivo experiments were performed on adult (8-week-old, 18–20 g) male C57BL/6J mice obtained from the Experimental Animal Center of Beijing Anzhen Hospital.

Generation and Characterization of β_1 -AA Monoclonal Antibody

β_1 -AA monoclonal antibody were generated by hybridoma technology, as we previously described.²³ Two peptides corresponding to the sequence (amino acid residues 197–223) of the second extracellular loop of the human β_1 -AR (peptide 1, H-W-W-R-A-E-S-D-E-A-R-R-C-Y-N-D-P-K-C-C-D-F-V-T-N-R-C; peptide 2, C-H-W-W-R-A-E-S-D-E-A-R-R; 98% purity,

Table 1. Hormonal and Metabolic Features of Study Subjects

Variable	Healthy Subjects	CAD Group	P Value
Sex ratio (women/men)	90:41	72:59	
Age, y	55.46±11.40	55.27±11.78	0.202
Glucose, mmol/L	5.22±0.66	6.52±2.14	<0.0001
HbA _{1C} , %	5.50±0.35	16.68±7.51	<0.0001
TCH, mmol/L	4.92±0.98	4.06±1.12	<0.0001
Triglyceride, mmol/L	1.36±0.81	1.80±1.72	0.07
LDL-C, mmol/L	2.93±0.85	2.23±1.01	<0.0001
HDL-C, mmol/L	1.41±0.46	1.07±0.27	<0.0001
C-reactive protein, mg/L	0.77±0.91	3.13±4.50	<0.01
AST, U/L	22±7.95	26.68±21.80	0.187
BNP, μg/L*	31.2±21.2 (5/131)	147.5±184.64 (22/131)	0.135
CK, U/L*	112.33±38.26 (5/131)	123.68±97.11	0.77
Whole blood MYO, ng/mL*	25.9±10.7 (2/131)	50.22±50.06 (19/131)	0.59
Whole blood troponin I, μg/L*	0.3 (1/42)	0.45±0.45 (12/131)	
CKMB, μg/L	†	15.17±14.65 (16/131)	
LDH, U/L	160.66±17.17	194.0±58.30	0.33
MMB, ng/mL*	0.95±0.28 (6/131)	1.71±1.22	0.13
TNI, ng/mL*	0.01 (2/131)	2.90±6.07 (24/131)	
β ₁ -AA (OD values)‡	0.32 (0.12–0.49)	0.86 (0.56–1.28)	<0.001

Data are given as mean±SD unless otherwise indicated. β₁-AA indicates autoantibodies against the second extracellular loop of β₁-adrenergic receptor; AST, aspartate aminotransferase; BNP, brain natriuretic peptide; CAD, coronary heart disease; CK, creatine kinase; CKMB, CK isoenzyme MB; HbA_{1C}, glycated hemoglobin; HDL-C, high-density lipoprotein cholesterol; LDH, lactate dehydrogenase; LDL-C, low-density lipoprotein cholesterol; OD, optical density; TCH, total cholesterol; TNI, troponin I; MYO, myoglobin; MMB,CK-MB mass.

*Data in parenthesis are number/total.

†The healthy control group did not test the CKMB index.

‡Data are given as median (interquartile range).

Qiang Yao, Shanghai Bio Scientific Commercial Development Co Ltd, China) were coupled to keyhole limpet hemocyanin. Three wild-type mice were immunized with 2 fusion peptides at the ratio of 2:1 (peptide 1:peptide 2). Splenocytes of 3 immunized wild-type mice were fused with the SP2/0 myeloma cell line at a ratio of 1:10. Hybridoma clones were tested by ELISA for production of antibodies against the 2 coupling peptides. Positive clones were cultivated in Iscove’s medium supplemented with 10% fetal calf serum, 2 mmol/L glutathione, 1 mmol/L sodium pyruvate, 100 UI/mL penicillin-streptomycin, and 50 mmol/L β-mercaptoethanol. Two wild-type mice were vaccinated with hybridoma cells secreting anti-β₁-AA monoclonal antibody (β₁-AAmAb). After 10 to 14 days, ascitic fluid from immunized mice was collected. IgGs were purified via protein G antibody affinity chromatography. Biolayer interferometry (BLI) technique and coimmunoprecipitation analysis were performed to detect the binding and affinity of β₁-AAmAb for β₁-AR on neonatal rat cardiac myocytes (NRVMs). Functional activity of β₁-AAmAb was tested by neonatal mouse cardiomyocytes’ beating frequency and intracellular cAMP accumulation.

BLI Binding Assay

Real-time binding assays between β₁-AAmAb/β₁-AA IgGs from patients with CAD and β₁-AR were performed using BLI with an Octet Red 96 instrument (Fortebio). In the BLI experiments, β₁-AR protein was biotinylated by the EZ-Link Sulfo-NHS-LC-Biotinylation kit (catalog No. 21435) from Thermo Scientific. Sulfo-NHS-LC-biotin was conjugated onto target proteins via the reaction between the NHS ester and the primary amino groups (including the N terminus of the protein and primary amines on the side chain of lysine) on proteins. Briefly, we incubated β₁-AR protein and Sulfo-NHS-LC-biotin at 1:1 molar ratio in double-distilled H₂O (600 μL volume), at 25°C for 40 minutes. After that, the excess free Sulfo-NHS-LC-biotin was removed by applying the protein sample to a desalting column (Zeba Spin Desalting Columns, 5 mL, for 500–2000-μL samples, 7000 molecular weight cutoff). After centrifugation of the column at 1000g for 2 minutes, the collected flow-through solution is the biotin-labeled β₁-AR protein for subsequent BLI experiments.

Biotinylated β₁-AR (in 20 mmol/L HEPES, pH 7.4, 150 mmol/L NaCl, and 1 mmol/L dithiothreitol) was first

Table 2. Hormonal and Metabolic Features of β₁-AA–Negative Group and β₁-AA–Positive Group

Variable	β ₁ -AA–Negative Group	β ₁ -AA–Positive Group	P Value
Sex ratio (women/men)	23:22	49:37	
Age, y	55.46±11.40	55.27±11.78	0.202
Glucose, mmol/L	7.72±2.43	7.49±2.55	0.05
HbA _{1c} , %	7.72±1.55	6.84±1.24	<0.05
TCH, mmol/L	3.96±1.06	4.10±0.59	0.8
Triglyceride, mmol/L	1.61±1.17	1.61±0.91	0.54
LDL-C, mmol/L	2.20±0.76	2.33±1.36	0.67
HDL-C, mmol/L	1.02±0.26	0.98±0.19	0.64
C-reactive protein, mg/L	1.87±1.36	3.25±3.02	<0.01
AST, U/L	23.55±12.80	30.77±13.01	0.08
BNP, μg/L*	140.30±101.51 (13/45)	182.42±59.30 (9/86)	0.3
CK, U/L	100.56±73.80	122.4±64.3	0.2
Whole blood MYO, ng/mL*	342.2±96.29 (11/45)	482.78±249.86 (8/86)	0.41
Whole blood troponin I, μg/L	0.25±0.18 (5/45)	0.15±0.11 (7/86)	0.2
CKMB, μg/L*	6.6±2.31 (5/45)	8.85±4.62 (11/86)	0.44
LDH, U/L	212.95±130.10	217.36±91.42	0.33
MMB, ng/mL	1.51±0.65	2.31±2.28	0.13
TNI, ng/mL*	0.13±0.11 (12/45)	0.34±0.36 (12/86)	0.26
β ₁ -AA (OD valves)	0.45 (0.32–0.58)	1.13 (0.81–1.54)	<0.001
CTRP9, ng/mL [†]	2.06 (1.60–2.43)	1.60 (0.86–2.30)	<0.01

Data are given as mean±SD unless otherwise indicated. β₁-AA indicates autoantibodies against the second extracellular loop of β₁-adrenergic receptor; AST indicates aspartate aminotransferase; BNP, brain natriuretic peptide; CK, creatine kinase; CKMB, CK isoenzyme MB; CTRP9, C1q tumor necrosis factor-related protein 9; HbA_{1c}, glycated hemoglobin; HDL-C, high-density lipoprotein; LDH, lactate dehydrogenase; LDL-C, low-density lipoprotein; OD, optical density; TCH, total cholesterol; TNI, troponin I.

*Data in parenthesis are number/total.

[†]Data are given as median (interquartile range).

immobilized onto streptavidin biosensors (ForteBio) at a speed of 111g for 4 minutes. The immobilized sensors were equilibrated in reaction buffer (20 mmol/L HEPES, pH 7.4, 150 mmol/L NaCl, 1 mmol/L dithiothreitol, and 0.02% Tween-20) at a speed of 4.44g for 3 minutes. Association curves were obtained by incubating a β₁-AR–coated biosensor with different concentrations of β₁-AAmAb or β₁-AA IgG solutions (1, 0.5, 0.25, or 0.125 μmol/L proteins in reaction buffer), the biosensor was rotated at a speed of 4.44g for 8 minutes, and dissociations were detected by incubating in reaction buffer without β₁-AAmAb or β₁-AA IgG proteins in the same condition. Data were acquired using an Octet Data Acquisition 7.0.1.17, according to the manufacturers' instructions. The assays were analyzed with the Octet Data Analysis Software 7.0.1.3.

Passive Immunization by β₁-AAmAb

Eight-week-old β₁-AA–negative wild-type mice were randomly subjected into the following groups: (1) vehicle group (n=8); (2) β₁-AAmAb group (n=8); and (3) CTRP9+β₁-AAmAb group

(n=8). Approximately 5 × 10¹¹ vg/mL rAAV9-cTnT-Full Ctrp9-FLAG viruses was diluted in 150 μL of normal saline and then injected into mice via the tail vein, to overexpress the cardiac-specific CTRP9. The construction of rAAV9-cTnT-Full Ctrp9-FLAG plasmid is provided in Data S1. Both β₁-AA and CTRP9+β₁-AA mice were intraperitoneally immunized with either β₁-AAmAb or saline (5 μg/g body weight) at day 0. Every 2 weeks thereafter until week 8, a booster injection of β₁-AAmAb (5 μg/g of body weight) was administered. Blood samples were collected before the intraperitoneal injection; sera were collected and stored at –80°C until further analysis.

ELISA

The titer of β₁-AA was measured by ELISA, and the results were expressed as optical density (OD) units according to the published methods.^{24,25} Briefly, the synthetic peptide (5 mg/mL in 100 mmol/L Na₂CO₃ [pH 11.0]) was coated onto the wells of microtiter plates and incubated overnight at 4°C. The wells were then saturated with 0.1% PMT (PBS bovine serum

albumin Tween) buffer (0.1% [w/v] albumin bovine V, 0.1% [v/v] Tween-20 in PBS, pH 7.4) for 1 hour at 37°C. After washing 3 times with Tween-20 in PBS, serial dilutions of human sera were added for 1 hour at 37°C. After washing 3 times, biotinylated goat-antihuman IgG antibodies (Sigma) at 1:1000 dilution in PMT were added and incubated for 1 hour at 37°C. After washing 3 times, streptavidin-peroxidase conjugate (Sigma) at 1:2000 dilution in the same buffer was added to the wells and incubated under the same conditions. Finally, 2,2-azino-di (3-ethylbenzothiazoline) sulfonic acid-H₂O₂ (Roche, Switzerland) substrate buffer was added and incubated for 30 minutes in the dark at room temperature. The OD values were measured at 405 nm by using a microplate reader (Spectra Max Plus; Molecular Devices). The antibody titer was calculated based on the ratio of OD values of positive/negative controls ($[\text{specimen OD} - \text{blank control OD}] / [\text{negative control OD} - \text{blank control OD}]$). Samples with β_1 -AA positive or negative were defined as positive/negative >2.1 or positive/negative <1.5 , respectively.

Quantification of CTRP9 in Serum Samples

The CTRP9 levels in the serum of cases and controls were detected by human CTRP9 ELISA kit (Aviscera Bioscience), according to manufacturer's instructions. Approximately 100 μ L of standard dilutions, serum, and positive control was added to each well and incubated on the plate shaker for 2 hours at room temperature. Subsequently, each well was aspirated and washed by filling each well with 1 \times wash buffer (300 μ L) using a squirt bottle. This step was repeated 3 times for a total of 4 washes. After that, 100 μ L of Detection Antibody working solution was added to each well, covered with plate sealer, and incubated on microplate shaker for 2 hours at room temperature. Then, each well was aspirated and washed, as described previously. After washing, 100 μ L of Streptavidin-HRP (Horseradish Peroxidase) Conjugate working solution was added to each well and incubated on microplate shaker for 45 minutes at room temperature. Each well was protected from light, and the aspiration/wash step was repeated. Later, 100 μ L of Substrate Solution was added to each well and incubated on microplate shaker for 8 minutes at room temperature in the dark. After incubation, 100 μ L of Stop Solution was added to each well. Finally, the OD of each well was measured within 15 minutes, by using a microplate reader with 450-nm wavelength filter.

Culture of Beating Neonatal Cardiomyocytes

NRVMs were isolated as described previously.²⁷ Briefly, newborn Wistar rats were disinfected with 70% ethanol and then euthanized by cervical dislocation. Hearts were excised and transferred to cold PBS, pH 7.2. The ventricles were

separated, minced gently by fine forceps, and digested in 0.25% trypsin solution (5 mL/heart) at 37°C for 25 minutes. The cell suspension was then centrifuged at 444g for 15 minutes at 4°C. Pellets were resuspended in growth medium (Dulbecco's modified Eagle's medium supplemented with 10% fetal bovine serum, 0.1% glutamine, and 0.1% antibiotic/antimycotic solution) and plated onto 6-well plates for 90 minutes at 37°C to eliminate fibroblasts (preplating step). Cells of the supernatant were collected and then replated onto a fresh 6-well plate. NRVMs were supplied with 2 mL growth medium per well with or without 10% fetal bovine serum and were incubated for 24 hours at 37°C in 5% CO₂. Subsequently, the cells were stimulated with β_1 -AA/IgG from patients with β_1 -AA-positive CAD (10^{-7} mol/L) for 48 hours.

The sera of 86 patients with β_1 -AA-positive CAD were prepared by MabTrap Kit (Amersham Bioscience, Sweden). The concentrations (mg/mL) and specificities of purified IgGs were determined by the Bicinchoninic Acid Protein Assay (Pierce) and ELISA, respectively. The number of beats of a selected isolated myocardial cell or a cluster of synchronously contracting cells in each of 10 fields was counted for 15 seconds each. The IgG fractions from patients with β_1 -AA-positive CAD and corresponding receptor agonists were added, and the cells were observed for 5 minutes after each addition. This procedure was repeated 3 times in different cultures to yield results representing a total of 30 cells or cell clusters.

Echocardiography

Transthoracic echocardiography Doppler examination was performed in a blinded manner by an experienced echocardiographer. The mice were lightly anesthetized with 2% isoflurane, shaved (chest only), and placed in a specially designed apparatus. Echocardiography was conducted using a High Resolution Imaging System Vevo 770 (Visual Sonics Inc, Canada) equipped with a 10-MHz phased array transducer. M-mode tracings were recorded at baseline (before immunization) and every 4 weeks thereafter, in the parasternal long- and short-axis views, through the aortic valve at the base of the aortic leaflets and through the anterior and posterior left ventricle (LV) wall at the papillary muscle level. Left ventricular ejection fraction and percentage fractional shortening were determined automatically in M mode by averaging the results from 3 consecutive heartbeats. The wall thickness and LV internal dimensions were measured on the screen (online), whereas the pulsed-wave Doppler spectra of mitral inflow and LV outflow were recorded from the apical 4- and 5-chamber views, respectively. Subsequently, the LV mass was assessed via modified cube formula equation. To ensure the reproducibility of mice echocardiographies, all

baseline examinations were repeated within 24 hours. To evaluate the accuracy of M-mode and Doppler (online) measurements, a second set of unmarked M-mode and Doppler images of each animal was stored digitally throughout the study.

Histology

The heart tissues from immunized mice were fixed with 10% neutral formaldehyde and dehydrated in graded ethanol (85%, 95%, and 100%). After xylene permeation, tissues were embedded in paraffin. The paraffin blocks were sectioned at 3- to 5- μ m thickness and mounted onto glass slides. Cardiac collagen content was assessed via Masson's trichrome staining.

Terminal Deoxynucleotidyl Transferase-Mediated dUTP Nick-End Labeling Staining

In situ cell death detection kit was applied to perform TdT-mediated dUTP nick end labeling (TUNEL) staining to evaluate apoptosis according to the protocol.²⁷ After PBS washing for 3 times, treated cardiomyocytes were fixed by 4% paraformaldehyde and permeabilized in 0.1% Triton X-100 sodium citrate buffer. Then, in situ cell death detection kits (Roche) were used to label apoptotic cells, and the nuclei were stained with 4',6-diamidino-2-phenylindole. Cells were imaged by fluorescence microscopy. The numbers of total cells and terminal deoxynucleotidyl transferase-mediated dUTP nick-end labeling-positive cells were automatically counted by Image-Pro plus version. The apoptosis rate was defined as ratio of apoptotic cells/total cells.

Lactate Dehydrogenase Assay

Heart tissue from mouse was homogenized, and lactate dehydrogenase activity was assessed using a Cytotoxicity Detection Kit (Roche Diagnostics Corporation, Indianapolis, IN).

Western Blot Analysis

Heart tissues were lysed by radioimmunoprecipitation assay lysis buffer (PPLYGEN, China) with fresh protease inhibitor of 0.1% phenylmethanesulfonyl fluoride (Solarbio). The protein concentration was measured using bicinchoninic acid assay with bovine serum albumin as the standard protein. Equal amounts of proteins (50 μ g) were separated in 10% SDS-polyacrylamide gels by electrophoresis. Proteins were transferred onto polyvinylidene difluoride membrane (Millipore) and probed with the specific primary antibody at 4°C overnight, followed by incubation with horseradish peroxidase-conjugated secondary antibody. The protein expression levels were determined by measuring the band intensities using Image Lab software (Bio-Rad).

Coimmunoprecipitation

Heart tissues were washed 2 times with PBS and lysed in buffer solution containing 10 mmol/L Tris-HCl (pH 7.4), 0.3 mol/L sucrose, 5 mmol/L EDTA, and proteinase inhibitor. Cell lysates were pipetted up and down with a 25-gauge syringe needle for 20 times on ice. Tissue debris was removed through centrifugation at 12 000g for 15 minutes at 4°C. Supernatant was transferred into a new Eppendorf tube, followed by 12 000g centrifugation for another 10 minutes at 4°C. A clear supernatant was obtained and incubated with protein agarose beads prebound with antibodies at 4°C for overnight. After washing with lysis buffer, beads were pelleted and suspended in SDS sample loading buffer. Supernatant proteins were separated by 10% SDS-PAGE and analyzed by Western blot.

Quantitative Real-Time Polymerase Chain Reaction

Total RNA was extracted from the frozen heart tissue by using Trizol reagent (Invitrogen). The concentrations and purities of total RNA were determined at 260 nm. The target genes were quantified by SYBR Premix Ex (Life Technologies), according to the manufacturer's instructions. Using the $2^{-\Delta\Delta C_t}$ method, the data were presented as the fold change in gene expression normalized to the endogenous reference gene (GAPDH) and relative to the untreated control. The primer sequences were as follows: mouse CTRP9, 5'-TGGTGA ACGTGGTGCCTACA-3' (forward) and 5'-TGCAGTCACATCCC ACCCT-3' (reverse); and mouse GAPDH, 5'-CCAGTATGACTC CACTCAGC-3' (forward) and 5'-GACTCCACGACATACTCAGC-3' (reverse).

cAMP Measurement

The level of cAMP was measured with Mouse cAMP ELISA Kit (Nanjing Jiancheng Bioengineering Institute, China). The heart tissues were weighted, added with PBS (pH 7.4), and completely homogenated with homogenizer. Supernatant was collected after centrifugation at 444g to 999g for 20 minutes. Before testing, the kit was stabilized for 30 minutes in ambient temperature. A total of 50 μ L diluted standard was added into standard well, 50 μ L standard/sample dilute was added into zero well, and 50 μ L sample was added into sample well. Then, 50 μ L biotinylated antibody working solution was added into each well. After sealing with closure plate membrane, the well plate was incubated for 60 minutes at 37°C. The 25 \times washing concentrate solution was diluted 25 times with distilled water for standby. The washing solution was added into each well and then discarded after stabilizing for 30 seconds. This step was repeated 5 times, and then pat dried. After that, 50 μ L

horseradish peroxidase working solution was added to standard well and sample wells, sealed with closure plate membrane, and then incubated at 37°C for 1 hour. After washing, 50 μ L chromogenic solution A was added into each well, followed by 50 μ L chromogenic solution B, and incubated for 10 minutes at 37°C in the dark. After incubation, 50 μ L stop solution was added into each well to stop the reaction. Finally, the OD of each well was measured under 450-nm wavelength.

Measurement of PKA Activity

PKA activity was measured using nonradioactive PepTag Assay (Promega, Madison, WI) dependent on a change in charge of the PepTag A1 peptide from +1 to -1 after phosphorylation.²⁸ Sample reaction mixtures were incubated for 1 minute in a water bath at 30°C. Then, the sample or cAMP-Dependent Protein Kinase, Catalytic Subunit was added and incubated at room temperature for 30 minutes. After incubation, the reactions were stopped by heating at 95°C for 10 minutes. The samples were then separated on a 0.8% (wt/vol) agarose gel at 100 V for 15 minutes. Purified PKA catalytic subunit was served as a positive control, whereas the negative control consisted of buffer only. Bands were visualized under Western Blotting Luminol Reagent system and autoradiography (Bio-Rad).

Statistical Analysis

Analyses were performed using SPSS 16.0 software (SPSS Inc, Chicago, IL). Data distribution was assessed using Shapiro-Wilk test. Normally distributed data were compared using the Student *t* tests or 1-way ANOVA. Nonnormally distributed unpaired data were compared using the Mann-Whitney *U* test or the Kruskal-Wallis test. Spearman test was used to report linear correlations between nonnormally distributed parameters. $P < 0.05$ was considered significant. Results were expressed as mean \pm SD for normally distributed data and as median \pm interquartile range (IQR) (25th–75th percentiles) for nonnormally distributed data.

Results

The Correlation Between CTRP9 Levels and β_1 -AA Levels

The levels of β_1 -AA and CTRP9 were detected by ELISA in sera collected from 131 patients with CAD and 131 healthy subjects. Serum titers of β_1 -AA were markedly increased in patients with CAD compared with healthy controls (0.32 [IQR, 0.12–0.49] versus 0.86 [IQR, 0.56–1.28]; $P < 0.001$; Figure 1A). Among the 131 patients with CAD, 86 of them were

positive for β_1 -AA, and the positive rate was significantly higher than for healthy individuals (65.6% versus 9.01%; Figure 1B). Notably, CTRP9 expression was significantly decreased (1.80 [IQR, 1.23–2.33] versus 2.12 [IQR, 1.78–2.82] ng/mL; $P < 0.001$; Figure 1C), and its levels in the β_1 -AA-positive group were significantly lower than in the β_1 -AA-negative group (1.60 [IQR, 0.86–2.30] versus 2.06 [IQR, 1.60–2.43] ng/mL; $P < 0.01$; Figure 1D). Spearman test demonstrated serum CTRP9 concentration was inversely correlated with β_1 -AA (Spearman $r = -0.31$, $P < 0.001$; Figure 1E). Taken together, there is a correlation between CTRP9 reduction and β_1 -AA levels.

β_1 -AAMAb Decreased the Levels of CTRP9 in Vitro and in Vivo

β_1 -AAMAbs produced by hybridoma technique bind with native β_1 -ARs and exert the same biological effects as β_1 -AAs circulating in patients with CAD (Figure S1). To further confirm the role of CTRP9 in β_1 -AAMAb-induced myocardial injury, a passive immunization mouse model was constructed. The results of ELISA indicated that the levels of β_1 -AA remained in mice over time, suggesting the establishment of a passive immunization mouse model (Figure S2A). As shown in Figure S2, the long-term existence of β_1 -AAMAb induced VR and worsened cardiac function. More important, the serum level of CTRP9 was lower in β_1 -AAMAb group than that in vehicle group (Figure 2A). The results of real-time polymerase chain reaction and Western blot assay demonstrated that the mRNA and protein levels of CTRP9 were decreased in β_1 -AA-positive mice (Figure 2B and 2C). Furthermore, we treated NRVMs with β_1 -AAMAb for 48 hours, and found that β_1 -AAMAb decreased the expression of CTRP9 in NRVMs compared with vehicle group (Figure 2D). Collectively, these data suggest that β_1 -AAMAb decreases the level of CTRP9.

Cardiac-Specific CTRP9 Overexpression Attenuated β_1 -AAMAb-Induced VR and Restored Cardiac Function

To verify whether CTRP9 reduction plays an important role in β_1 -AAMAb-induced VR, AAV9 (Adeno-associated virus9)-mediated cardiac-specific CTRP9 overexpression model was constructed. As shown in Figure 3A and Figure S3A, CTRP9 was specifically overexpressed in the heart. At the eighth week of passive immunization, echocardiographic assessment revealed an increase in ejection fraction and fractional shortening in cardiac-specific CTRP9 overexpression mice compared with β_1 -AAMAb treatment alone (ejection fraction: 79.13 \pm 0.83% versus 65.21 \pm 0.23%; fractional shortening: 46.61 \pm 0.74% versus 34.98 \pm 0.49%; $P < 0.001$; Figure 3B and

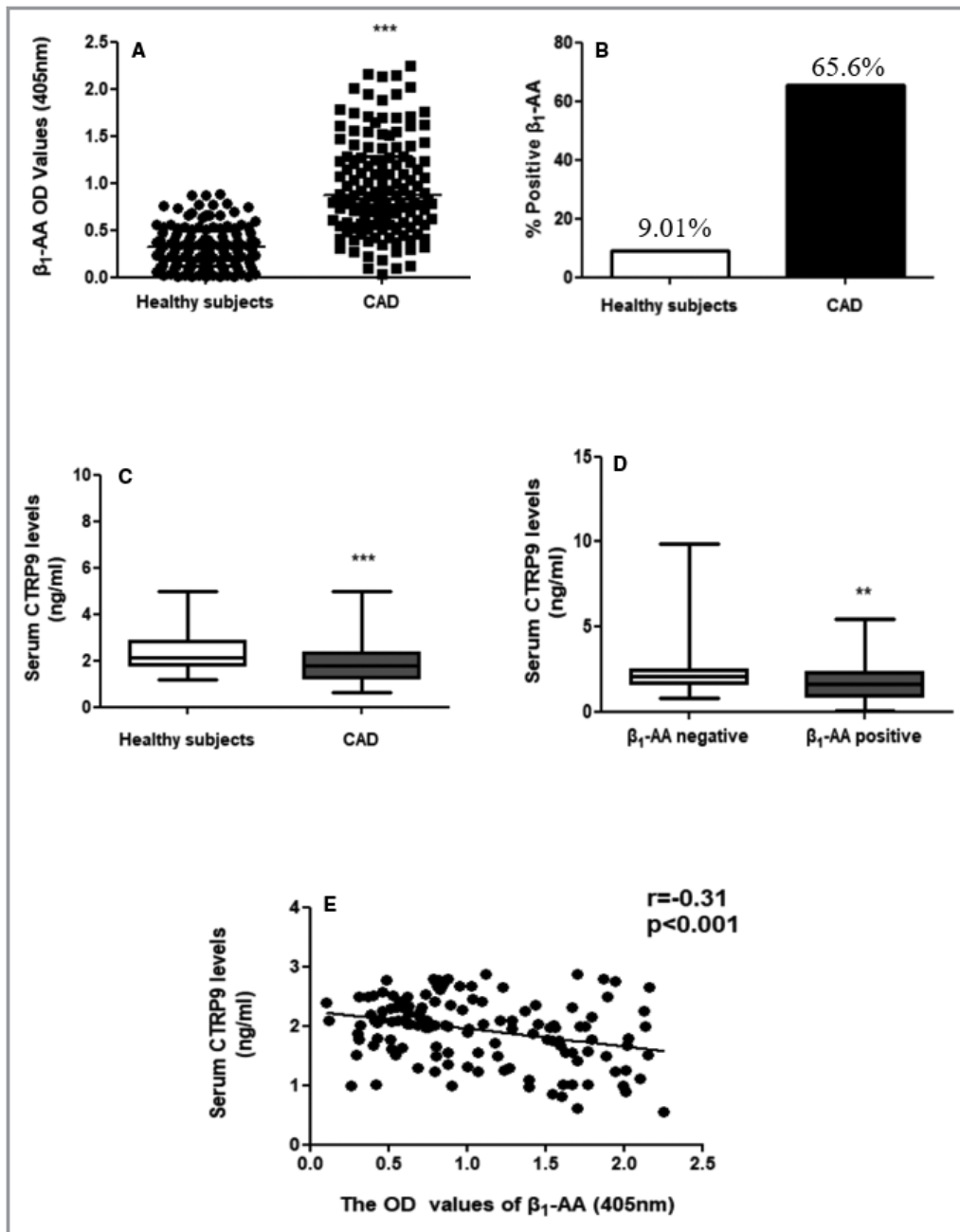


Figure 1. The correlation between CTRP9 (C1q tumor necrosis factor-related protein 9) levels and autoantibodies against the second extracellular loop of β_1 -adrenergic receptor (β_1 -AA) levels. **A**, Serum titers of β_1 -AA in healthy subjects and patients with coronary heart disease (CAD). **B**, The positive rate of β_1 -AA in healthy subjects and patients with CAD. **C**, Circulating CTRP9 levels in healthy subjects and patients with CAD. **D**, Circulating CTRP9 levels in β_1 -AA–positive group (n=86) and β_1 -AA–negative group (n=45). **E**, Serum CTRP9 concentrations were inversely correlated with β_1 -AA (n=131, $r = -0.31$). Data are presented as mean \pm SD or median \pm interquartile range (25th–75th percentile). OD indicates optical density. ** $P < 0.01$, *** $P < 0.001$.

3C). Similarly, left ventricular diastolic diameter (3.12 ± 0.09 versus 3.53 ± 0.01 mm; $P < 0.001$) and left ventricular systolic diameter (1.76 ± 0.07 versus 2.30 ± 0.02 mm; $P < 0.001$) were decreased in AAV9-CTRP9–treated mice (Figure 3D and 3E). Moreover, cardiac-specific CTRP9

overexpression significantly suppressed interstitial fibrosis (Figure 4A and 4B) and decreased matrix metalloproteinase-2/matrix metalloproteinase-9 expressions, the 2 most significant mechanisms contributing to cardiac fibrosis (Figure 4C and 4D). In addition, CTRP9 overexpression dramatically

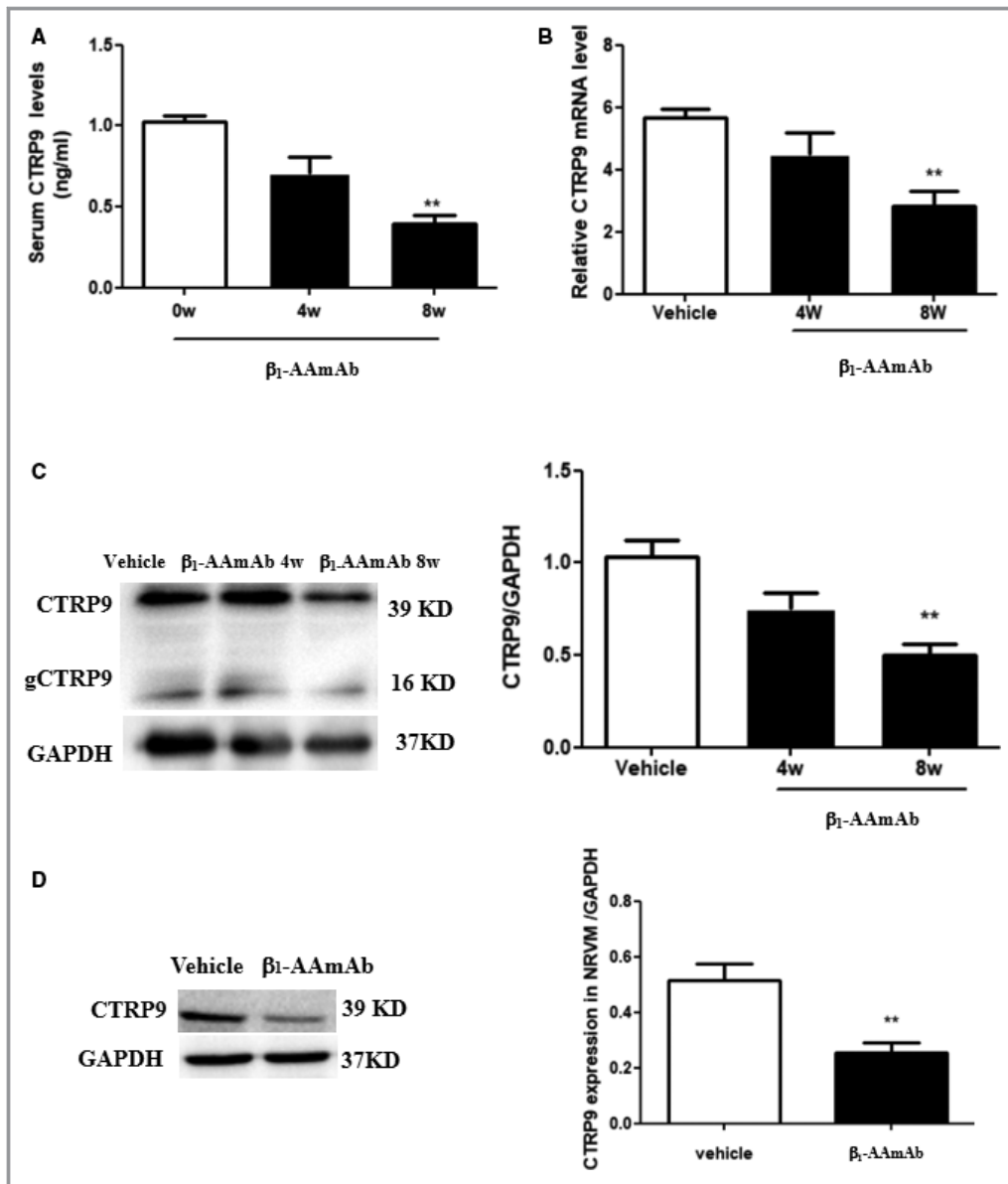


Figure 2. Autoantibodies against the second extracellular loop of β₁-adrenergic receptor monoclonal antibodies (β₁-AAmAbs) decreased the levels of CTRP9 (C1q tumor necrosis factor-related protein 9) in vitro and in vivo. **A**, Serum CTRP9 levels. **B**, The mRNA expression levels CTRP9 (normalized to GAPDH). Vehicle is for 8 weeks. **C**, Western blot analysis for CTRP9 expression. Vehicle is for 8 weeks. **D**, Western blot analysis for CTRP9 expression in neonatal rat cardiomyocytes (NRVMs) in the presence of β₁-AAmAbs (10⁻⁷ mol/L, 48 hours). n=8. 4w indicates fourth week after immunization; 8w, eighth week after immunization; gCTR9, globular CTRP9. **P<0.01 vs before immunization (0 week) or vehicle group.

attenuated cleaved caspase-3 expression (Figure 5A) and reduced the number of terminal deoxynucleotidyl transferase-mediated dUTP nick-end labeling-positive cells (Figure 5C), but no change was observed in full-length caspase-3 expression (Figure 5B). Furthermore, β₁-AAmAb-mediated increase in lactate dehydrogenase level was also significantly reduced in CTRP9-treatment mice (Figure 5D). These data suggest that AAV9-mediated cardiac-specific CTRP9 overexpression protects against VR induced by β₁-AAmAb.

CTR9 Overexpression Reversed the G-Protein-Coupled Receptor Kinase 2/AdipoR1/AMPK Pathway

cAMP/PKA is a classic signaling pathway that exerts physical and pathological effects. Previous studies indicated β₁-AA enhanced the proliferation of T lymphocytes and cardiac fibroblasts and induced the apoptosis of cardiomyocytes in vitro and in vivo through cAMP/PKA pathway.²⁹⁻³¹

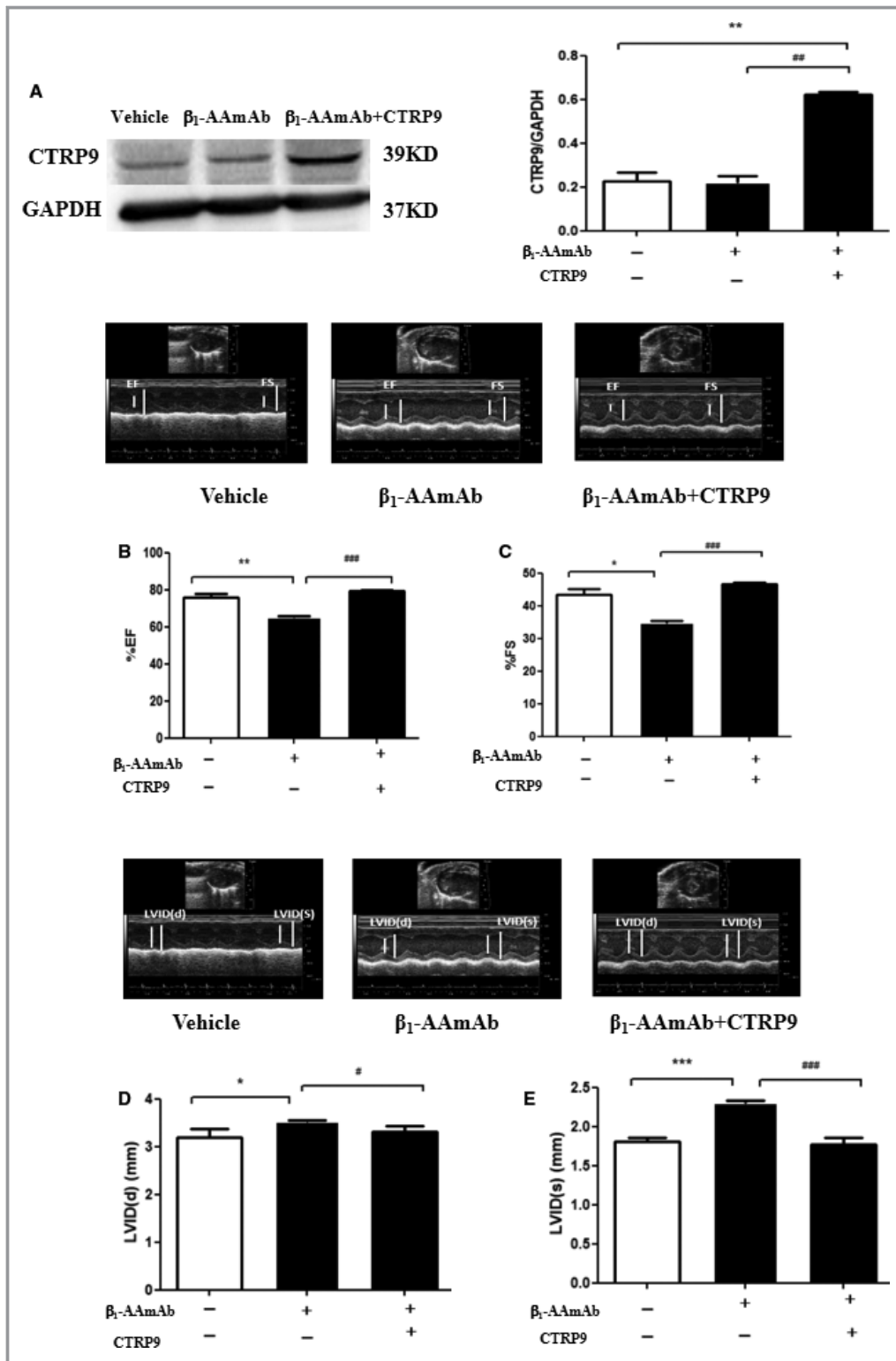


Figure 3. CTRP9 (C1q tumor necrosis factor-related protein 9) overexpression restored cardiac function. **A**, Western blot analysis for CTRP9 expression in vehicle, autoantibodies against the second extracellular loop of β₁-adrenergic receptor monoclonal antibody (β₁-AAb), and β₁-AAb+CTRP9 groups. **B**, Echocardiographic left ventricular ejection fraction (EF) of mice. **C**, Echocardiographic left ventricular fractional shortening (FS) of mice. **D**, Echocardiographic left ventricular inner dimension of diastolic (LVID [d]). **E**, Echocardiographic left ventricular inner dimension of systolic (LVID[s]). n=8 in each group. *P<0.05, **P<0.01, ***P<0.001 vs vehicle; #P<0.05, ##P<0.01, ###P<0.001 vs β₁-AAb group.

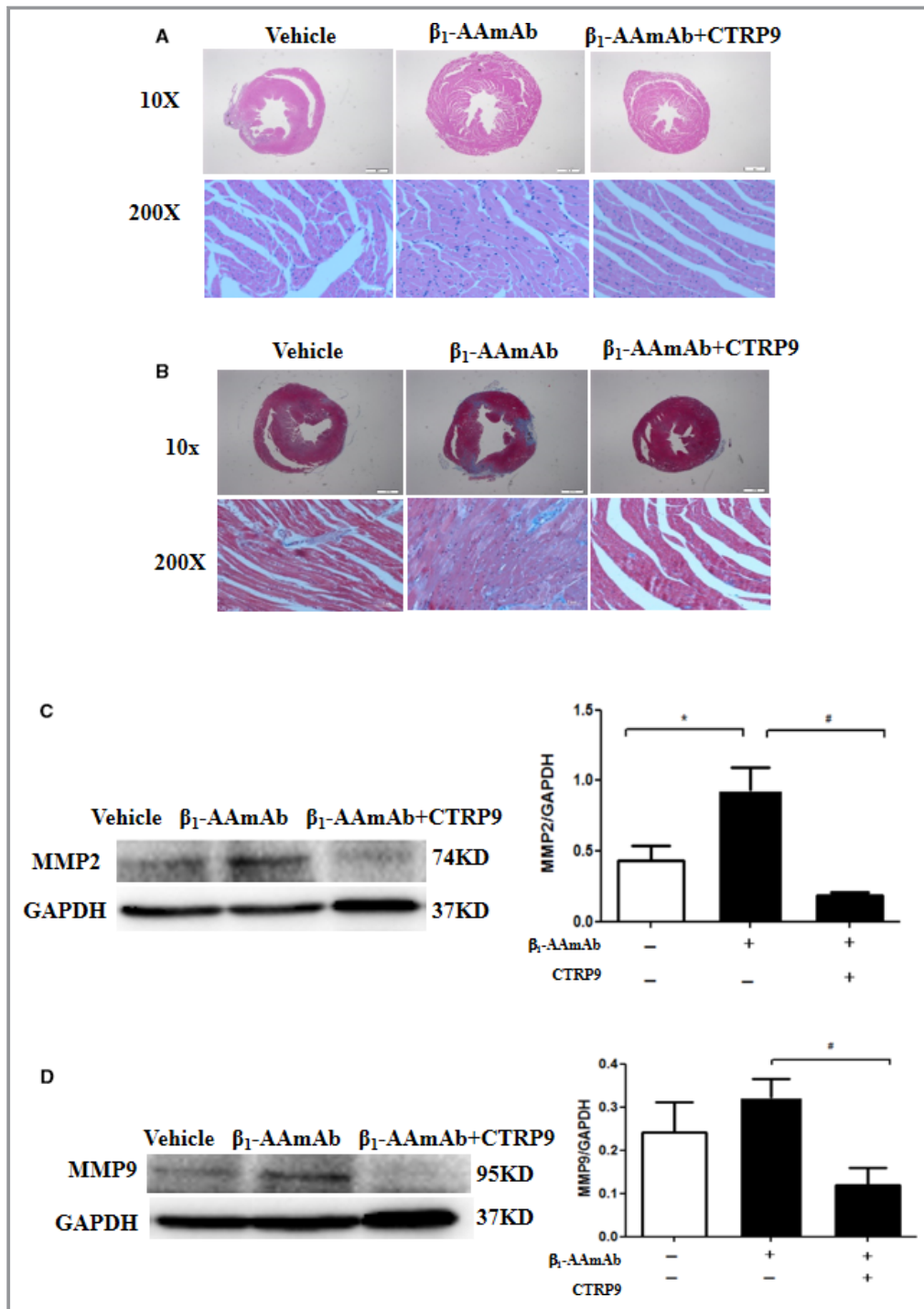


Figure 4. CTRP9 (C1q tumor necrosis factor-related protein 9) overexpression attenuated autoantibodies against the second extracellular loop of β_1 -adrenergic receptor monoclonal antibody (β_1 -AAmAb)-induced ventricular remodeling. **A**, Hematoxylin-eosin staining. **B**, Masson's trichrome staining. **C**, Western blot analysis for matrix metalloproteinase-2 (MMP2) expression. **D**, Western blot analysis for MMP9 expression. n=8 in each group. * P <0.05 vs vehicle; # P <0.05 vs β_1 -AAmAb group.

Therefore, we investigated whether the cAMP/PKA pathway is involved in β_1 -AAmAb-induced VR. The results showed compared with vehicle group, the levels of cAMP and PKA phosphorylation as well as PKA activity were increased in

β_1 -AAmAb group (Figure 6A through 6C), suggesting that cAMP/PKA pathway is activated in β_1 -AAmAb-induced VR.

AdipoR1 is the main receptor of CTRP9.²¹ A recent study reported that AdipoR1 is phosphorylatively modified and

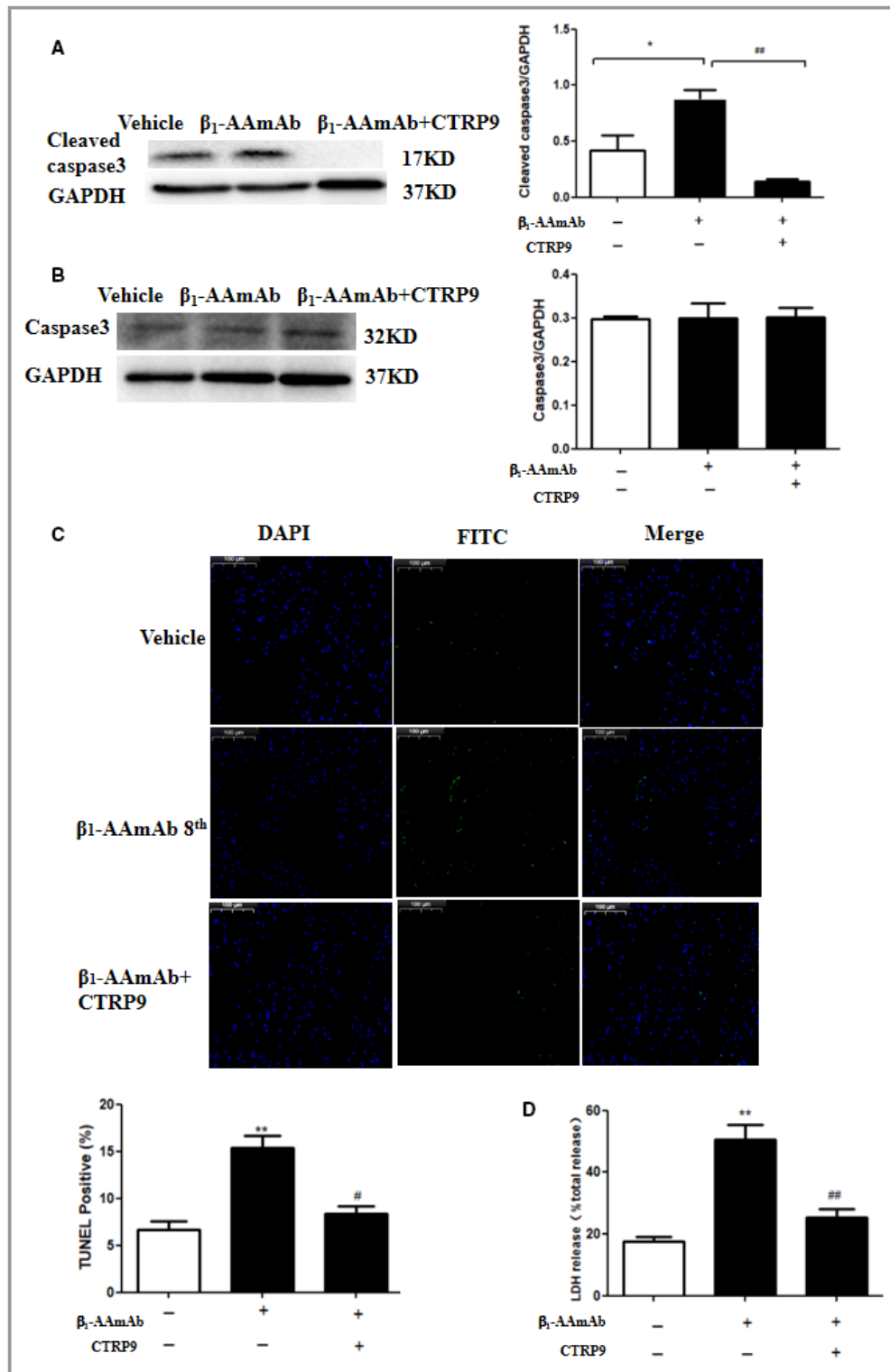


Figure 5. CTRP9 (C1q tumor necrosis factor-related protein 9) overexpression attenuated autoantibodies against the second extracellular loop of β₁-adrenergic receptor monoclonal antibody (β₁-AAmAb)-induced apoptosis and necrosis. **A**, Western blot analysis for cleaved caspase-3 expression. **B**, Western blot analysis for full-length caspase-3 expression. **C**, Terminal deoxynucleotidyl transferase-mediated dUTP nick-end labeling (TUNEL) staining. **D**, Lactate dehydrogenase (LDH) level. n=8 per group. DAPI indicates 4',6-diamidino-2-phenylindole; FITC, fluorescein isothiocyanate. *P<0.05, **P<0.01 vs vehicle; #P<0.05, ##P<0.01 vs β₁-AAmAb group.

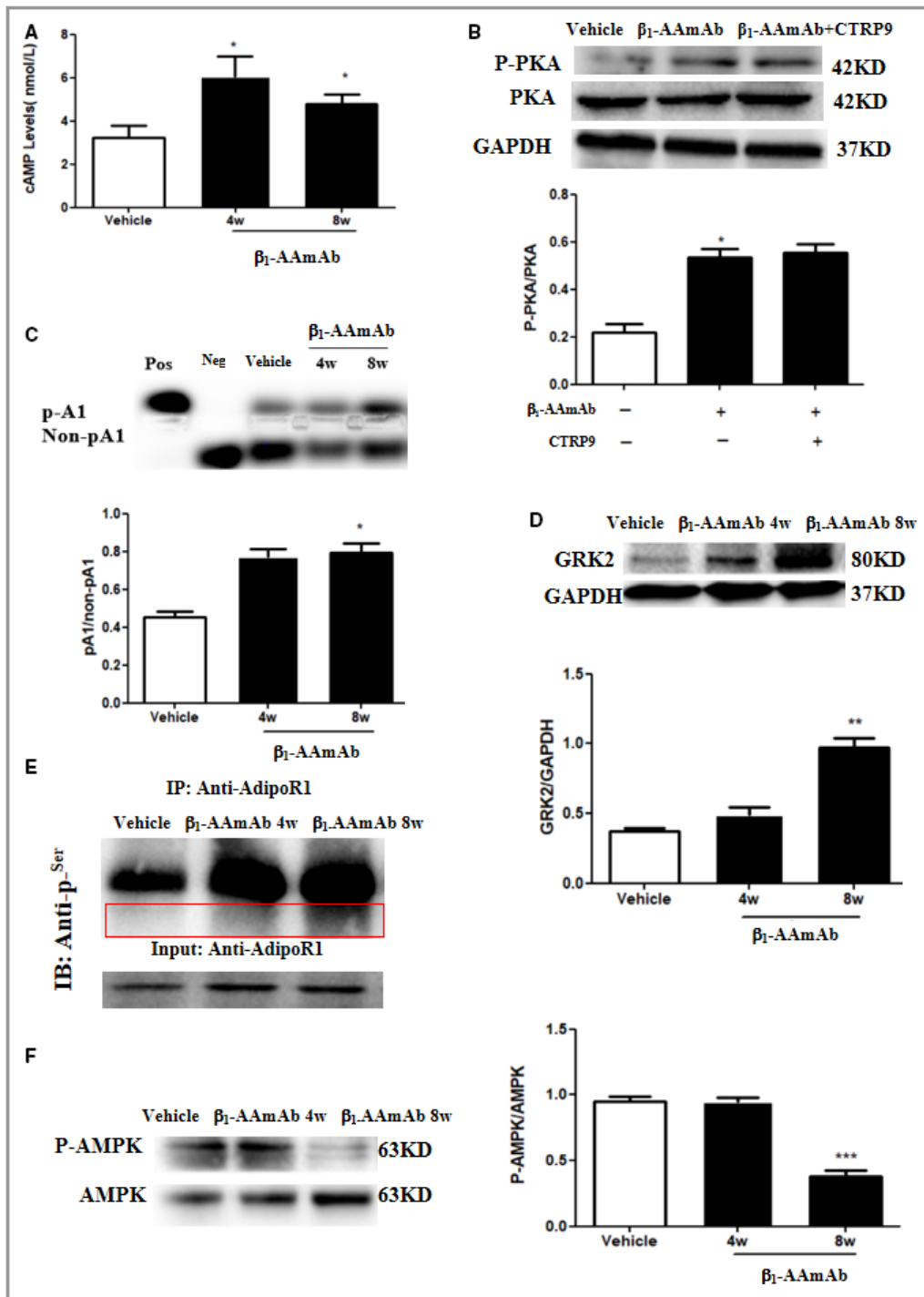


Figure 6. Both cAMP/protein kinase A (PKA) and G-protein–coupled receptor kinase (GRK)/adiponectin receptor 1 (AdipoR1)/AMP-activated protein kinase (AMPK) pathways were activated in autoantibodies against the second extracellular loop of β₁-adrenergic receptor monoclonal antibody (β₁-AAmAb) group. **A**, cAMP levels. **B**, The phosphorylation levels of PKA (P-PKA). **C**, PKA activity. **D**, Western blot analysis for GRK expression. **E**, Coimmunoprecipitation for AdipoR1 phosphorylation. **F**, Western blot analysis for the expression and phosphorylation of AMPK (P-AMPK). n=8. 4w indicates fourth week after immunization; 8w, eighth week after immunization; CTRP9, C1q tumor necrosis factor-related protein 9; IB, immunoblot; IP, immunoprecipitation; Neg, negative; Non-pA1, nonphosphorylated PepTag A1 peptide; p-A1, phosphorylated PepTag A1 peptide; Pos, positive. **P*<0.05, ***P*<0.01, ****P*<0.001.

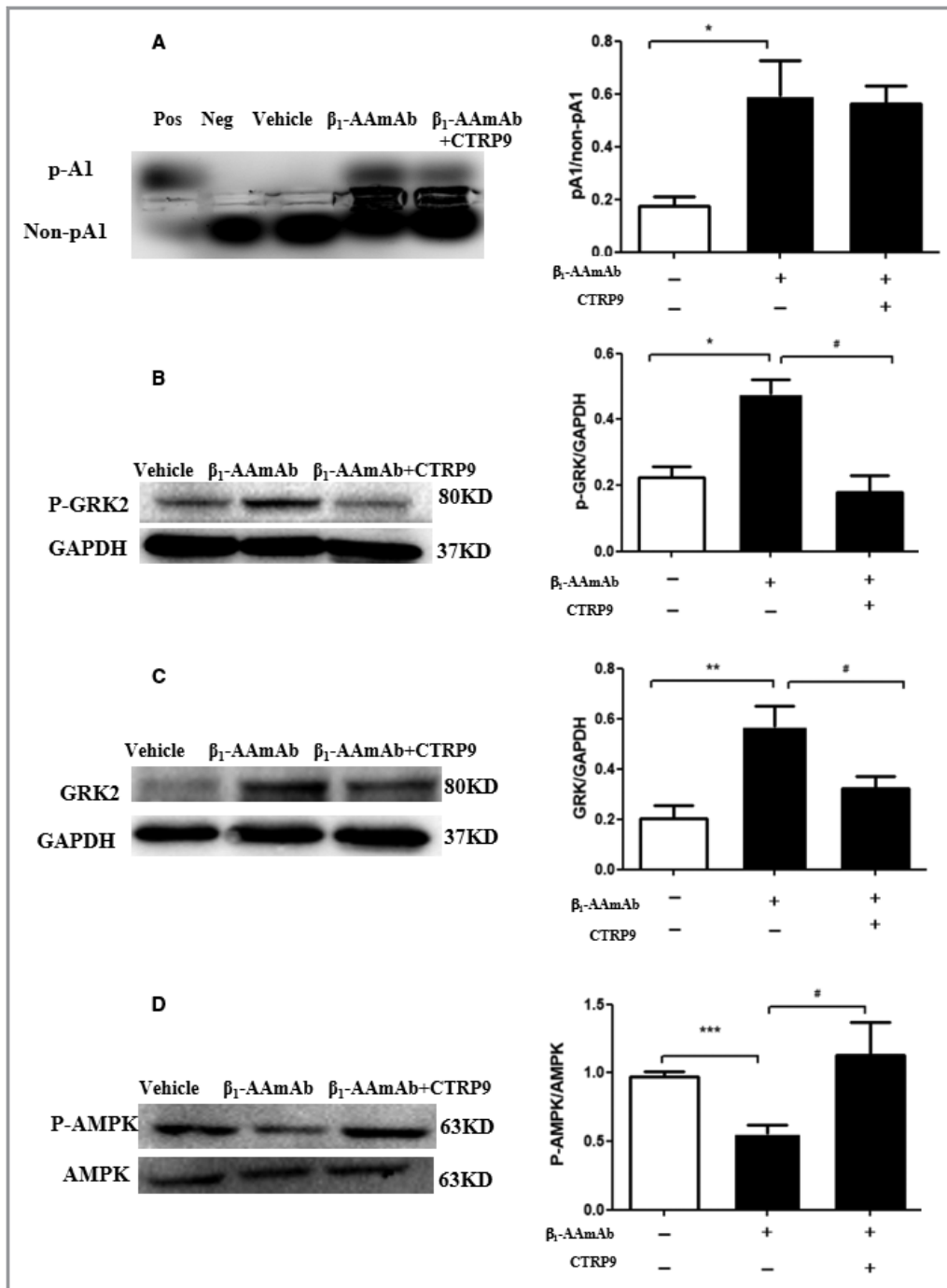


Figure 7. CTRP9 (C1q tumor necrosis factor-related protein 9) overexpression regulated G-protein-coupled receptor kinase 2 (GRK2)/adiponectin receptor 1/AMP-activated protein kinase pathway. **A**, Protein kinase A activity. **B** and **C**, The phosphorylation and expression levels of GRK (p-GRK). **D**, The phosphorylation levels of AMPK. n=8 in each group. β₁-AAmAb indicates autoantibodies against the second extracellular loop of β₁-adrenergic receptor monoclonal antibody; Neg, negative; Non-pA1, nonphosphorylated PepTag A1 peptide; p-A1, phosphorylated PepTag A1 peptide; Pos, positive. *P<0.05, **P<0.01, ***P<0.001 vs vehicle; #P<0.05 vs β₁-AAmAb group.

desensitized by G-protein-coupled receptor kinase 2 (GRK2) in failing cardiomyocytes, which contributes to post-myocardial infarction remodeling and HF progression.³² Moreover, exacerbated cardiac fibrosis induced by β-adrenergic

activation is caused by the decreased AMPK activity,³³ and AMPK as downstream of AdipoR1 can protect against acute myocardial injury.²¹ Therefore, in this study, the expression and phosphorylation levels of GRK2, AdipoR1, and AMPK were

detected, to examine the role of GRK2/AdipoR1/AMPK pathway in β_1 -AA-induced VR. Our findings demonstrated that β_1 -AAmAb increased GRK2 expression (Figure 6D) and AdipoR1 phosphorylation (Figure 6E), but the activity of AMPK was inhibited (Figure 6F). Collectively, these results suggest that GRK2/AdipoR1/AMPK pathway is involved in β_1 -AAmAb-induced VR.

In addition, we investigated the effects of CTRP9 on both cAMP/PKA and GRK2/AdipoR1/AMPK pathways. There was no significant change in phosphorylation level of PKA and PKA activity in CTRP9 overexpression mice (Figures 6B and 7A). However, the phosphorylation and expression levels of GRK2 were inhibited by CTRP9 (Figure 7B and 7C). As shown in Figure 7D, CTRP9 activated AMPK, evidenced by the increased phosphorylation of the AMPK α -subunit. Taken altogether, these results demonstrate that the CTRP9 rescued β_1 -AAmAb-induced VR via GRK2/AdipoR1/AMPK pathway.

Discussion

The current study showed that the long-term existence of β_1 -AAmAb induced VR and decreased CTRP9 levels in vitro and in vivo. Cardiac-specific overexpressed CTRP9 ameliorated the β_1 -AAmAb-induced VR and restored heart function. Furthermore, by exploring the underlying mechanisms, we found that GRK2/AdipoR1/AMPK pathway played an important role in CTRP9-rescued VR.

Many reports have demonstrated that the concentration of circulating β_1 -AA was increased in patients with HF compared with healthy subjects.^{14,15} The present study confirmed the findings, in which β_1 -AA was detected in 65.6% of sera collected from 131 patients with CAD, which was significantly higher than in 131 healthy subjects. In addition, our animal experiments revealed that the cardiac fibrosis was increased in β_1 -AAmAb passive immunization mouse model and the cardiac function was reduced at the eighth week. Therefore, we further explored the mechanisms underlying β_1 -AA-induced VR.

Previously, β_1 -AAs were obtained from the sera of β_1 -AA-positive patients³⁴ or active β_1 -AR-EC_{II} (the second extracellular loop of 1-adrenergic receptor) immunized animals.³⁵ Because β_1 -AAs act in concert with other GPCR (G-protein-coupled receptor) autoantibodies in patients with HF, and IgG fractions also included nonspecific IgGs, they were not specific for the second extracellular loop of β_1 -AR. Other kinds of antibodies might have interfered with the effects of β_1 -AA. Moreover, we also tried to purify specific β_1 -AA from patients with cardiac disease through affinity column. However, because only 5 mL of venous blood was collected from an ethical point of view, the concentration of purified β_1 -AA was too low to conduct in vivo experiments. Therefore, herein, we obtained a monoclonal antibody against β_1 -AR-EC_{II} using

hybridoma technology to eliminate the interference of non-specific IgGs. Coimmunoprecipitation analysis and BLI technique were performed to detect the binding and affinity of β_1 -AAmAb for β_1 -AR. The results indicated that “synthetic” β_1 -AAmAb specifically bound to β_1 -AR on NRVMs. In addition, similar to the function of IgGs from β_1 -AA-positive patients, β_1 -AAmAb also increased the beating rate of NRVMs and cAMP level (Figures S1 and S4). Therefore, we decided to further our research by also using the β_1 -AAmAbs to determine the role of CTRP9 in VR induced by β_1 -AA. Furthermore, β_1 -AAmAb is injected into the body as a kind of IgG, which produces a small amount of anti- β_1 -AA antibodies. As the concentration of β_1 -AAmAb in the body increases, the titers of anti- β_1 -AA antibodies may also increase. However, because β_1 -AA and anti- β_1 -AA antibodies are homologous, traditional antibody detection methods, such as ELISA, are unable to detect the concentration of anti- β_1 -AA antibody, and it is also difficult to conduct a functional analysis. According to reports in the literature, time-resolved based homogeneous assays have been used widely in research and diagnosis to detect antibodies, disease markers, and receptor-ligand binding.^{36,37} Therefore, in the further study, we will use the time-resolved FRET (Fluorescence Resonance Energy Transfer)-based approach to detect the concentrations of anti- β_1 -AA antibody and further separate the anti- β_1 -AA antibody using BLI to analyze its function.³⁸

Recently, the concept that the heart acted as a secretory organ has drawn increasing attention. Proteins secreted by the heart are included “cardiokines,”^{16,39} and they play a critical physiological role in maintaining heart homeostasis and respond to myocardial damage, leading to the development of cardiac diseases. A previous study demonstrated that CTRP9 is not a typical adipokine but instead functions as a potent cardioprotective cardiokine, which is highly expressed in the adult heart.¹⁸ It has been reported that CTRP9 supplementation protects the heart from ischemic injury and attenuates the adverse cardiac remodeling after ischemic myocardial infarction.^{19,21,22} Moreover, plasma CTRP9 levels are significantly reduced after myocardial ischemia/reperfusion injury,¹⁹ and serum CTRP9 levels were dramatically decreased in patients with CAD compared with patients without CAD.⁴⁰ These findings suggest that reduced CTRP9 plays an important role in myocardial injury.

In this study, we found a lower CTRP9 level in patients with CAD compared with healthy controls. According to the titers of β_1 -AA, patients with CAD were divided into β_1 -AA-positive group and β_1 -AA-negative group. We found that the level of CTRP9 in β_1 -AA-positive group was lower than that in β_1 -AA-negative group and the concentration of CTRP9 was inversely correlated with β_1 -AA. However, the correlation between the 2 groups was weak. We consider this may be related to the clinical samples used in our study. According to reports in the

literature, CTRP9 is a cardioprotective cardiokine, which plays a stronger role in HF caused by myocardial ischemia/reperfusion and acute myocardial infarction.^{18,21} However, animal experiments demonstrated that the long-term presence of β_1 -AA mainly induces cardiac insufficiency instead of HF.^{30,31} Therefore, to match the pathological model induced by β_1 -AA, patients with acute myocardial infarction and congestive HF were excluded, and only patients with CAD were included in our study. Even so, we found that the levels of CTRP9 in β_1 -AA-positive group were significantly lower than in β_1 -AA-negative group, suggesting that β_1 -AA positivity was related to CTRP9 levels. Moreover, to investigate the role of cardiokine CTRP9 in β_1 -AAMAb-induced VR and to further analyze the causal relationship between the 2 groups, *in vitro* and *in vivo* experiments were performed. The results showed that β_1 -AAMAb directly decreased the expression of CTRP9 and cardiac-specific overexpressed CTRP9 ameliorated the β_1 -AAMAb-induced VR and restored heart function. Therefore, we believe CTRP9 plays an important role in β_1 -AAMAb-induced VR and the reduction of CTRP9 is a direct effect of β_1 -AA not attributable to congestive heart failure and VR.

Adiponectin, a 30-kDa protein that is produced mainly by mature adipocytes, has been implicated in a wide spectrum of biological pathways related to peripheral insulin sensitivity,⁴¹ inflammatory response,^{41,42} and cardiovascular diseases.⁴³ It has been suggested that adiponectin can play a protective role at an early phase of myocardial infarction.⁴³ Moreover, reduced adiponectin levels are correlated with increased risk of acute myocardial infarction,⁴⁴ and worsen cardiac functional recovery after myocardial infarction with reperfusion.^{45,46} In addition, there is clear experimental evidence demonstrating a link between adiponectin deficiency and HF progression.⁴⁷⁻⁴⁹ Therefore, in this study, we examined the levels of adiponectin after β_1 -AAMAb passive immunization. Our results indicated a nonsignificant change of adiponectin level in heart tissues (Figure S5B). Adiponectin was once considered as a major adipocyte-secreted protein, which is highly expressed in adipose tissues. However, CTRP9 is the most highly expressed cardiokine in the heart, exceeding the expression of adiponectin by >100-fold.²² Therefore, we believed that the reduced CTRP9, but not adiponectin, might be involved in β_1 -AA-induced VR.

The structure of CTRP9 consists of 4 distinct domains: a signal peptide at the N terminus, a short variable region, a collagenous domain, and a C-terminal globular domain, which is homologous to adiponectin.⁵⁰ In contrast to adiponectin that circulates as full-length multimers, CTRP9 circulates primarily in the globular domain isoform (gCTRP9). Recombinant full-length CTRP9 was cleaved to produce gCTRP9, a process that was inhibited by protease inhibitor cocktail. gCTRP9 rapidly activates cardiac survival kinases, including AMPK and protein kinase B. These findings support that

CTRP9 undergoes proteolytic cleavage to generate gCTRP9, the dominant circulatory and actively cardioprotective isoform.⁵¹ We next demonstrated the important role of CTRP9 in VR induced by β_1 -AA. Treatment with gCTRP9 increases systemic CTRP9 levels, but not cardiac-specific CTRP9 levels. Thus, we intravenously injected the mice with a CTRP9 encoding AAV9 vector (rAAV9-cTnT promoter-Full Ctrp9-FLAG), to overexpress CTRP9 in the heart tissues. Compared with β_1 -AAMAb treatment, AAV9-CTRP9-treated mice showed increases in ejection fraction and fractional shortening, and decreases in cardiac fibrosis and apoptosis, suggesting that CTRP9 may ameliorate VR induced by β_1 -AA.

cAMP/PKA pathway is the most common signaling mechanism initiated by β_1 -AR stimulation.^{52,53} Previous studies have indicated that β_1 -AA can enhance the proliferation of T lymphocytes²⁹ and cardiac fibroblasts,³⁰ and induce cardiomyocyte apoptosis *in vitro* and *in vivo* through the modulation of cAMP/PKA pathway.²⁰ In this study, we found that the cAMP/PKA pathway was activated by β_1 -AA at eighth week of passive immunization. However, overexpression of CTRP9 had no effect on cAMP/PKA pathway, suggesting that this pathway is not regulated by CTRP9 in the β_1 -AA-induced VR.

AdipoR1 and AdipoR2, 2 structurally related 7 transmembrane receptors, have been identified as the functional receptors for adiponectin.⁵⁴ AdipoR1 is abundantly expressed in the heart,⁵⁵ whereas AdipoR2 is predominantly found in liver.⁵⁶ Moreover, AdipoR1 may be the main receptor of CTRP9,²¹ and is not phosphorylated in the normal heart. AdipoR1 is phosphorylatively modified and desensitized by GRK2 in failing cardiomyocytes, which contributes to post-myocardial infarction remodeling and HF progression.³⁰ Our study demonstrated an increased phosphorylation of AdipoR1 and upregulation of GRK2 expression during β_1 -AAMAb stimulation. However, there was no change in the relative phosphorylation of AdipoR2 (Figure S5C). A recent study has reported that metformin can improve the survival of patients with HF,⁵⁷ supporting that the pharmacologic activation of AMPK may be beneficial in HF treatment. Moreover, the prolonged (isoproterenol) stimulation can inhibit AMPK activation and induce subsequent cell apoptosis in cardiomyocytes, suggesting that inactivation of AMPK may play an important role in myocardial injury.⁵⁸ In this study, we found that the long-term existence of β_1 -AAMAb can decrease the phosphorylation of AMPK. Furthermore, CTRP9 overexpression reduced the levels of GRK2 and promoted the activation of AMPK. Taken together, our data suggest that VR is modulated by the reduced CTRP9 via AdipoR1/GRK2/AMPK pathway.

In summary, the present study demonstrates that CTRP9 level is decreased in VR induced by β_1 -AAMAb. However, the mechanisms by which β_1 -AAMAb induced the reduction of CTRP9 are not well understood, which may serve as a new direction for future research.

Disclosures

None.

References

- Ziaeian F. Epidemiology and aetiology of heart failure. *Nat Rev Cardiol*. 2016;13:368–78.
- Kacimi R, Gerdes AM. Alterations in G protein and MAP kinase signaling pathways during cardiac remodeling in hypertension and heart failure. *Hypertension*. 2003;41:968–977.
- Wallukat G, Wollenberger A. Effects of the serum gamma globulin fraction of patients with allergic asthma and dilated cardiomyopathy on chronotropic beta adrenoceptor function in cultured neonatal rat heart myocytes. *Biomed Biochim Acta*. 1987;46:S634–S639.
- Wallukat G, Reinke P, Dörrfel WV, Luther HP, Bestvater K, Felix SB, Baumann G. Removal of autoantibodies in dilated cardiomyopathy by immunoadsorption. *Int J Cardiol*. 1996;54:191–195.
- Fu Y, Xiao H, Zhang Y. Beta-adrenoceptor signaling pathways mediate cardiac pathological remodeling. *Front Biosci*. 2012;4:1625–1637.
- Buwall L, Täng MS, Isic A, Andersson B, Fu M. Antibodies against the beta1-adrenergic receptor induce progressive development of cardiomyopathy. *J Mol Cell Cardiol*. 2007;42:1001–1007.
- Fan Y, Chen Y, Wan Z, Zhou D, Ma A. The prognostic value of autoantibodies against β 1-adrenoceptor and cardiac troponin-I for clinical outcomes in STEMI. *J Cardiovasc Med*. 2017;18:34–41.
- Chan V, Fenning A, Hoey A, Brown L. Chronic β -adrenoceptor antagonist treatment controls cardiovascular remodeling in heart failure in the aging spontaneously hypertensive rat. *J Cardiovasc Pharmacol*. 2011;58:424–431.
- Magnusson Y, Marullo S, Hoyer S, Waagstein F, Andersson B, Vahlne A, Guillet JG, Strosberg AD, Hjalmarson A, Hoebeke J. Mapping of a functional autoimmune epitope on the beta 1-adrenergic receptor in patients with idiopathic dilated cardiomyopathy. *J Clin Invest*. 1990;86:1658–1663.
- Magnusson Y, Wallukat G, Waagstein F, Hjalmarson A, Hoebeke J. Autoimmunity in idiopathic dilated cardiomyopathy: characterization of antibodies against the beta 1-adrenoceptor with positive chronotropic effect. *Circulation*. 1994;89:2760–2767.
- Jahns R, Boivin V, Lohse MJ. beta(1)-Adrenergic receptor function, autoimmunity, and pathogenesis of dilated cardiomyopathy. *Trends Cardiovasc Med*. 2006;16:20–24.
- Patel PA, Hernandez AF. Targeting anti-beta-1-adrenergic receptor antibodies for dilated cardiomyopathy. *Eur J Heart Fail*. 2013;15:724–729.
- Dandel M, Wallukat G, Potapov E, Hetzer R. Role of β 1-adrenoceptor autoantibodies in the pathogenesis of dilated cardiomyopathy. *Immunobiology*. 2012;217:511–520.
- Bornholz B, Roggenbuck D, Jahns R, Boege F. Diagnostic and therapeutic aspects of β 1-adrenergic receptor autoantibodies in human heart disease. *Autoimmun Rev*. 2014;13:954–962.
- Boivin-Jahns V, Jahns R, Boege F. Relevant effects of beta1-adrenoceptor autoantibodies in chronic heart failure. *Front Biosci*. 2018;23:2146–2156.
- Doroudgar S, Glembotki CC. The cardiokine story unfolds: ischemic stress-induced protein secretion in the heart. *Trends Mol Med*. 2011;17:207–214.
- Bax NA, van Marion MH, Shah B, Goumans MJ, Bouten CV, van der Schaft DW. Matrix production and remodeling capacity of cardiomyocyte progenitor cells during in vitro differentiation. *J Mol Cell Cardiol*. 2012;53:497–508.
- Yan W, Guo Y, Tao L, Lau WB, Gan L, Yan Z, Guo R, Gao E, Wong GW, Koch WL, Wang Y, Ma XL. C1q/tumor necrosis factor-related protein-9 regulates the fate of implanted mesenchymal stem cells and mobilizes their protective effects against ischemic heart injury via multiple novel signaling pathways. *Circulation*. 2017;136:2162–2177.
- Kambara T, Ohashi K, Shibata R, Ogura Y, Maruyama S, Enomoto T, Uemura Y, Shimizu Y, Yuasa D, Matsuo K, Miyabe M, Kataoka Y, Murohara T, Ouchi N. CTRP9 protein protects against myocardial injury following ischemia-reperfusion through AMP-activated protein kinase (AMPK)-dependent mechanism. *J Biol Chem*. 2012;287:18965–18973.
- Su H, Yuan Y, Wang XM, Lau WB, Wang Y, Wang X, Gao E, Koch WJ, Ma XL. Inhibition of CTRP9, a novel and cardiac-abundantly expressed cell survival molecule, by TNF α -initiated oxidative signaling contributes to exacerbated cardiac injury in diabetic mice. *Basic Res Cardiol*. 2013;108:315.
- Kambara T, Shibata R, Ohashi K, Matsuo K, Hiramatsu-Ito M, Enomoto T, Yuasa D, Ito M, Hayakawa S, Ogawa H, Aprahamian T, Walsh K, Murohara T, Ouchi N. C1q/tumor necrosis factor-related protein 9 protects against acute myocardial injury through an adiponectin receptor I-AMPK-dependent mechanism. *Mol Cell Biol*. 2015;35:2173–2185.
- Sun Y, Yi W, Yuan Y, Lau WB, Yi D, Wang X, Wang Y, Su H, Wang X, Gao E, Koch WJ, Ma XL. C1q/tumor necrosis factor-related protein-9, a novel adipocyte-derived cytokine, attenuates adverse remodeling in the ischemic mouse heart via protein kinase A activation. *Circulation*. 2013;10:128.
- Gong Y, Xiong H, Du Y, Wu Y, Zhang S, Li X, Liu H. Autoantibodies against 1-adrenoceptor induce blood glucose enhancement and insulin insufficient via T lymphocytes. *Immunol Res*. 2016;64:584–93.
- Jahns R, Boivin V, Siegmund C, Inselmann G, Lohse MJ, Boege F. Autoantibodies activating human beta1-adrenergic receptors are associated with reduced cardiac function in chronic heart failure. *Circulation*. 1999;99:649–654.
- Holthoff HP, Zeibig S, Jahns-Boivin V, Bauer J, Lohse MJ, Käbb S, Claus S, Jahns R, Schlipp A, Münch G, Ungerer M. Detection of anti- β 1-AR autoantibodies in heart failure by a cell-based competition ELISA. *Circ Res*. 2012;111:675–684.
- Goebel A, Giricz Z, Szunyog A, Csont T, Burley DS, Baxter GF, Ferdinandy P. Role of cGMP-PKG signaling in the protection of neonatal rat cardiac myocytes subjected to simulated ischemia/reoxygenation. *Basic Res Cardiol*. 2010;105:643–650.
- Fan K, Li D, Zhang Y, Han C, Liang J, Hou C, Xiao H, Ikenaka K, Ma J. The induction of neuronal death by up-regulated microglial cathepsin H in LPS-induced neuroinflammation. *J Neuroinflammation*. 2015;12:54.
- Khalilulin I, Parker JE, Halestrap AP. Consecutive pharmacological activation of PKA and PKC mimics the potent cardioprotection of temperature preconditioning. *Cardiovasc Res*. 2010;88:324–333.
- Du Y, Yan L, Wang J, Zhan W, Song K, Han X, Li X, Cao J, Liu H. β 1-Adrenoceptor autoantibodies from DCM patients enhance the proliferation of T lymphocytes through the β 1-AR/cAMP/PKA and p38 MAPK pathways. *PLoS One*. 2012;7:e52911.
- Lv T, Du Y, Cao N, Zhang S, Gong Y, Bai Y, Wang W, Liu H. Proliferation in cardiac fibroblasts induced by β 1-adrenoceptor autoantibody and the underlying mechanisms. *Sci Rep*. 2016;6:32430.
- Jane-Wit D, Altuntas CZ, Johnson JM, Yong S, Wickley PJ, Clark P, Wang Q, Popović ZB, Penn MS, Damron DS, Perez DM, Tuohy VK. Beta 1-adrenergic receptor autoantibodies mediate dilated cardiomyopathy by agonistically inducing cardiomyocyte apoptosis. *Circulation*. 2007;116:399–410.
- Wang Y, Gao E, Lau WB, Wang Y, Liu G, Li JJ, Wang X, Yuan Y, Koch WJ, Ma XL. G-protein-coupled receptor kinase 2-mediated desensitization of adiponectin receptor 1 in failing heart. *Circulation*. 2015;131:1392–1404.
- Wang J, Song Y, Li H, Shen Q, Shen J, An X, Wu J, Zhang J, Wu Y, Xiao H, Zhang Y. Exacerbated cardiac fibrosis induced by β -adrenergic activation in old mice due to decreased AMPK activity. *Clin Exp Pharmacol Physiol*. 2016;43:1029–1037.
- Buwall L, Bollano E, Chen J, Shultz W, Fu M. Phenotype of early cardiomyopathic changes induced by active immunization of rats with a synthetic peptide corresponding to the second extracellular loop of the human beta-adrenergic receptor. *Clin Exp Immunol*. 2006;143:209–215.
- Zuo L, Bao H, Tian J, Wang X, Zhang S, He Z, Yan L, Zhao R, Ma XL, Liu H. Long-term active immunization with a synthetic peptide corresponding to the second extracellular loop of β 1-adrenoceptor induces both morphological and functional cardiomyopathic changes in rats. *Int J Cardiol*. 2011;149:89–94.
- Wegner KD, Lanth PT, Jennings T, Oh E, Jain V, Fairclough SM, Smith JM, Giovanelli E, Lequeux N, Pons T, Hildebrandt N. Influence of luminescence quantum yield, surface coating, and functionalization of quantum dots on the sensitivity of time-resolved FRET bioassays. *ACS Appl Mater Interfaces*. 2013;5:2881–2892.
- Blomberg K, Hurskainen P, Hemmälä I. Terbium and rhodamine as labels in a homogeneous time-resolved fluorometric energy transfer assay of the beta subunit of human chorionic gonadotropin in serum. *Clin Chem*. 1999;45:855–861.
- Sun T, Reid F, Liu Y, Cao Y, Estep P, Nauman C, Xu Y. High throughput detection of antibody self-interaction by bio-layer interferometry. *MAbs*. 2013;5:838–841.
- Shimano M, Ouchi N, Walsh K. Cardiokines: recent progress in elucidating the cardiac secretome. *Circulation*. 2012;126:e327–e332.
- Wang J, Hang T, Cheng XM, Li DM, Zhang QG, Wang LJ, Peng YP, Gong JB. Associations of C1q/TNF-related protein-9 levels in serum and epicardial adipose tissue with coronary atherosclerosis in humans. *Biomed Res Int*. 2015;2015:971683.
- Yamauchi T, Nio Y, Maki T, Kobayashi M, Takazawa T, Iwabu M, Okada-Iwabu M, Kawamoto S, Kubota N, Kubota T, Ito Y, Kamon J, Tsuchida A, Kumagai K, Kozono H, Hada Y, Ogata H, Tokuyama K, Tsunoda M, Ide T, Murakami K, Awazawa M, Takamoto I, Froguel P, Hara K, Tobe K, Nagai R, Ueki K, Kadowaki T. Targeted disruption of AdipoR1 and AdipoR2 causes abrogation of adiponectin binding and metabolic actions. *Nat Med*. 2007;13:332–339.

42. Ouchi N, Kihara S, Arita Y, Nishida M, Matsuyama A, Okamoto Y, Ishigami M, Kuriyama H, Kishida K, Nishizawa H, Hotta K, Muraguchi M, Ohmoto Y, Yamashita S, Funahashi T, Matsuzawa Y. Adipocyte-derived plasma protein, adiponectin, suppresses lipid accumulation and class A scavenger receptor expression in human monocyte-derived macrophages. *Circulation*. 2001;103:1057–1063.
43. Kalisz M, Baranowska B, Wolinska-Witort E, Maczewski M, Mackiewicz U, Tulacz D, Gora M, Martynska L, Bik W. Total and high molecular weight adiponectin levels in the rat model of post-myocardial infarction heart failure. *J Physiol Pharmacol*. 2015;66:673–680.
44. Pischon T, Girman CJ, Hotamisligil GS, Rifai N, Hu FB, Rimm EB. Plasma adiponectin levels and risk of myocardial infarction in men. *JAMA*. 2004;291:1730–1737.
45. Shibata R, Numaguchi Y, Matsushita K, Sone T, Kubota R, Ohashi T, Ishii M, Kihara S, Walsh K, Ouchi N, Murohara T. Usefulness of adiponectin to predict myocardial salvage following successful reperfusion in patients with acute myocardial infarction. *Am J Cardiol*. 2008;101:1712–1715.
46. Shibata R, Sato K, Pimentel DR, Takemura Y, Kihara S, Ohashi K, Funahashi T, Ouchi N, Walsh K. Adiponectin protects against myocardial ischemia-reperfusion injury through AMPK- and COX-2-dependent mechanisms. *Nat Med*. 2005;11:1096–1103.
47. Liao Y, Takashima S, Maeda N, Ouchi N, Komamura K, Shimomura I, Hori M, Matsuzawa Y, Funahashi T, Kitakaze M. Exacerbation of heart failure in adiponectin-deficient mice due to impaired regulation of AMPK and glucose metabolism. *Cardiovasc Res*. 2005;67:705–713.
48. Shimano M, Ouchi N, Shibata R, Ohashi K, Pimentel DR, Murohara T, Walsh K. Adiponectin deficiency exacerbates cardiac dysfunction following pressure overload through disruption of an AMPK-dependent angiogenic response. *J Mol Cell Cardiol*. 2010;49:210–220.
49. Shibata R, Izumiya Y, Sato K, Papanicolaou K, Kihara S, Colucci WS, Sam F, Ouchi N, Walsh K. Adiponectin protects against the development of systolic dysfunction following myocardial infarction. *J Mol Cell Cardiol*. 2007;42:1065–1074.
50. Zhang SH, Du YH, Yu HC, Li YM, Liu HR. Research advances in the regulation of cardiovascular metabolic disorders and its related risk factors by C1q/TNF related proteins. *Sheng Li Xue Bao*. 2018;70:310–318.
51. Yuan Y, Lau WB, Su H, Sun Y, Yi W, Du Y, Christopher T, Lopez B, Wang Y, Ma XL. C1q-TNF-related protein-9, a novel cardioprotective cardiokine, requires proteolytic cleavage to generate a biologically active globular domain isoform. *Am J Physiol Endocrinol Metab*. 2015;308:E891–E898.
52. Tutor AS, Penela P, Mayor F Jr. Anti- β 1-adrenergic receptor autoantibodies are potent stimulators of the ERK1/2 pathway in cardiac cells. *Cardiovasc Res*. 2007;76:51–60.
53. Chiale PA, Rosenbaum MB, Elizari MV, Hjalmarsen A, Magnusson Y, Wallukat G, Hoebeke J. High prevalence of antibodies against beta-1 and beta-2 adrenoceptors in patients with primary electrical cardiac abnormalities. *J Am Coll Cardiol*. 1995;26:864–869.
54. Achari AE, Jain SK. Adiponectin, a therapeutic target for obesity, diabetes, and endothelial dysfunction. *Int J Mol Sci*. 2017;18:1321.
55. Kim JT, Kim Y, Cho YM, Koo BK, Lee EK, Shin HD, Jang HC, Choi JW, Oh B, Park KS. Polymorphisms of ADIPOR1 and ADIPOR2 are associated with phenotypes of type 2 diabetes in Koreans. *Clin Endocrinol*. 2009;70:66–74.
56. Yamauchi T, Kamon J, Ito Y, Tsuchida A, Yokomizo T, Kita S, Sugiyama T, Miyagishi M, Hara K, Tsunoda M, Murakami K, Ohteki T, Uchida S, Takekawa S, Waki H, Tsuno NH, Shibata Y, Terauchi Y, Froguel P, Tobe K, Koyasu S, Taira K, Kitamura T, Shimizu T, Nagai R, Kadowaki T. Cloning of adiponectin receptors that mediate antidiabetic metabolic effects. *Nature*. 2003;423:762–769.
57. Gundewar S, Calvert JW, Jha S, Toedt-Pingel I, Ji SY, Nunez D, Ramachandran A, Anaya-Cisneros M, Tian R, Lefer DJ. Activation of AMP-activated protein kinase by metformin improves left ventricular function and survival in heart failure. *Circ Res*. 2009;104:403–411.
58. Zhuo XZ, Wu Y, Ni YJ, Liu JH, Gong M, Wang XH, Wei F, Wang TZ, Yuan Z, Ma AQ, Song P. Isoproterenol instigates cardiomyocyte apoptosis and heart failure via AMPK inactivation-mediated endoplasmic reticulum stress. *Apoptosis*. 2013;18:800–810.

1 **Supplemental Materials**

2 **Supplemental methods (Data S1)**

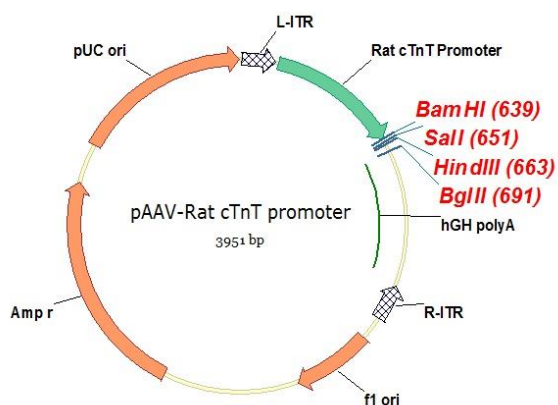
3 **pAAV-cTnT promoter-Full Ctrp9-FLAG Plasmid construction**

4 Gene Name: Full Ctrp9

5 Cloning Vector: pAAV-Rat cTnT promoter

6 Cloning Strategy: Sall+BglII

7 Vector Map:



8

9 Rat cTnT promoter sequence: 497bp

10 CGTGTGGCTGTTACAGTTGGCTTCTCTCAAGCGACTGCTTGAGAATGTAAT
11 AGTCGTTTATCTCTTCTAGTGGTTGAGTTCCACGCTGGGGAGGGCCCCAGT
12 TCTTGCCACCGGTTCCCTCAGGGGAGCTCAGTGGCAGGATGAAAATATCCAG
13 TGAGAAAAGAAAGGGGGCGCTGTTCACTAGAACTCTCTGCTCCCCTGAAA
14 AGTGGAGAAGCAGGGTTAACCTTTCTTTGAGGAATACAAATACGAACGAA
15 GTCTAGGGTGGCATGCCCGCTCAGGGGCAGGGAACGGGGAACACCAGTTG
16 GCCATCTCGGTGTGATGCAGGCGTTGAGGTTGCTTCCTTGCGGAGGAGGAA
17 ACGAGCATTCTACTGTGGGCCACACAGGGGATTCACCCCCAGGCCTCTGA
18 ATTCTAGCTGGGTGCAGAGGGCTCCGGTGGGAGGCAGCCTTCTCTCCTCAC

19 CCGCAGTGATGATTTTCTCTTTCTGGAGGGAGAACGGAGAAC
20 Full Ctrp9-3×FLAG sequence: 1068bp
21 ATGAGGATTTGGTGGCTTCTGCTGGTTATGGGTGCATGCACGAGAAGTGTAT
22 TCTCCCAGGACACCTGCCGGCAAGGGCACTCCGGCATCCCTGGGAATCCA
23 GGTCACAATGGCCTACCTGGAAGAGATGGACGAGATGGTGCCAAGGGTGA
24 CAAAGGAGACGCAGGAGAACCAGGACATCCTGGTGGTCCAGGAAAGGAT
25 GGAATTCGTGGGGAGAAAGGAGAACCAGGAGCAGATGGAAGAGTTGAAG
26 CAAAAGGCATCAAAGGTGATCCAGGCTCCAGAGGATCTCCGGGGAAACAT
27 GGCCCAAAGGGATCCATTGGTCCTACAGGAGAGCAAGGGCTGCCAGGAGA
28 GACTGGCCCTCAGGGGCAGAAGGGGGATAAAGGCGAAGTGGGCCCCACT
29 GGACCCGAAGGACTAATGGGCAGTACTGGTCCTTTGGGTCCCAAGGGCTTA
30 CCTGGCCCGATGGGCCCCATCGGCAAACCAGGTCCCAGGGGAGAAGCTGG
31 ACCCATGGGCCCCCAGGGGGAGCCAGGAGTCAGAGGAATGAGAGGCTGG
32 AAAGGCGATCGAGGAGAGAAGGGGAAAGTTGGTGAGGCTCCCCTTGTGCC
33 CAAGAGTGCTTTCCTACTGTGGGACTCACGGTGATCAGTAAGTTCCTCCCCC
34 AGATGCACCCATTAATTCGATAAGATCCTATAACAATGAACTGAACCACTAC
35 AATGTAGCGACGGGGAAGTTCACCTGCCACGTGGCAGGTGTCTATTACTTT
36 ACCTACCATATCACTGTGTTCTCCAGGAATGTGCAGGTATCTTTGGTCAAAA
37 ACGGGGTAAAAGTCCTGCACACCAAGGACAGTTACATGAGCTCTGAGGAC
38 CAGGCGTCTGGTGGCATTGTGCAGGAGCTGAAACTCGGGGACGAAGTGTG
39 GATGCAGGTGACAGGAGGAGAGAGGTTCAATGGCTTATTTGCAGACGAGG
40 ATGACGATACCACGTTACGGGCTTCCTGCTGTTTCAGCAGCTCTGACTACA

41 AAGACCATGACGGTGATTATAAAGATCATGACATCGATTACAAGGATGACG

42 ATGACAAGTGA

43 1)DNA primers synthesized: Full-Ctrp9-SalI-F:

44 5'-CGCGTCGACGCCACCATGAGGATTTGGTGGCTTCTGCTGG-3', Ctrp9-R1:

45 5'-

46 CATGATCTTTATAATCACCGTCATGGTCTTTGTAGTCAGAGCTGCTGAACAG

47 CAGGAAG-3', Ctrp9-BglII-R2:

48 5'-

49 GGAAGATCTCACTTGTCATCGTCATCCTTGTAATCGATGTCATGATCTTTATA

50 ATCAC-3'. 2) Using the plasmid ctrp9 as a template, the target gene full ctrp9 was

51 amplified by PCR, and the restriction sites of SalI and BglII were introduced at both

52 ends of the primers. The full ctrp9 DNA band (1068 bp) was recovered using 1%

53 agarose gel. 3) The vector pAAV-rat cTnT promoter and the PCR production full ctrp9

54 were digested with SalI+BglII in a 37 °C for 3 hours, while the large fragment and the

55 full ctrp9 fragment of vector pAAV-rat cTnT promoter were recovered. 4) Vector

56 pAAV-rat cTnT promoter SalI+BglII and full Ctrp9 fragment were linked at 22 °C for 3

57 hours. 5) Approximately 10µl of the connection product and 100µl of JM109 competent

58 bacteria were mixed, followed by ice bathing for 30 min and heat-shocked at 42 °C for

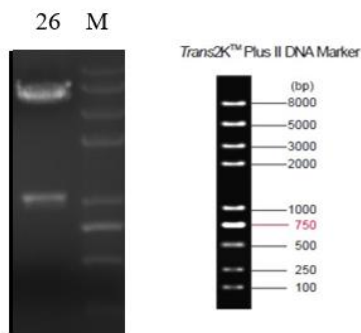
59 45 s. After that, the mixture immediately placed on ice for 2 min, added with 400µl LB

60 medium, and cultured at 37 °C for 1 hour with shaker. After 4000 rpm centrifugation

61 for 1 min, 400µl of the culture supernatant was discarded, while the remaining 100µl

62 was uniformly mixed by pipetting and spread evenly on an LB plate containing 100

63 $\mu\text{g/ml}$ ampicillin resistance. The plate was incubated overnight in an incubator at 37 °C.
 64 6) Four single colonies were selected and inoculated into LB culture medium containing
 65 5 ml of 100 $\mu\text{g/ml}$ Ampicillin resistance. Cells were cultured overnight in a constant
 66 temperature shaker at 250 rpm, 37 °C. The plasmid was extracted with plasmid
 67 extraction kit, followed by enzyme digestion and subjected to DNA sequencing. The
 68 results of plasmid digestion showed that the 26# clone was a positive clone.



69

70 Plasmid pAAV-cTnT promoter-Full Ctrp9-FLAG Sall+BglII digestion

71 Lane M: Trans2K plus marker

72 Full-ctrp9-26_HGH-R

73 CATGACTACAGGTTGTCTTCCCAACTTGCCCCTTGCTCCATACCACCCCCCT
 74 CCACCCCAT AATATTATAGAAGGACACCTAGTCAGACAAAATGATGCAACTT
 75 AATTTTATTAGGACAAGGCTGGTGGGCACTGGAGTGGCAACTTCCAGGGCC
 76 AGGAGAGGCACTGGGGAGGGGTCACAGGGATGCCACCCGTAGATCTCACT
 77 TGTCATCGTCATCCTTGTAATCGATGTCATGATCTTTATAATCACCGTCATGG
 78 TCTTTGTAGTCAGAGCTGCTGAACAGCAGGAAGCCCGTGAACGTGGTATCG
 79 TCATCCTCGTCTGCAAATAAGCCATTGAACCTCTCTCCTCCTGTCACCTGCA
 80 TCCACACTTCGTCCCCGAGTTTCAGCTCCTGCACAATGCCACCAGACGCCT
 81 GGTCTCAGAGCTCATGTA ACTGTCCTTGGTGTGCAGGACTTTTACCCCGTT

82 TTTGACCAAAGATACCTGCACATTCCTGGAGAACACAGTGATATGGTAGGT
83 AAAGTAATAGACACCTGCCACGTGGCAGGTGAACTTCCCCGTCGCTACATT
84 GTAGTGGTTCAGTTCATTGTATAGGATCTTATCGAATTTAATGGGTGCATCTG
85 GGGGAGGGAACTTACTGATCACCGTGAGTCCCACAGTGAAAGCACTCTTG
86 GGCACAAGGGGAGCCTCACCAACTTTCCCCTTCTCTCCTCGATCGCCTTTC
87 CAGCCTCTCATTCTCTGACTCCTGGCTCCCCCTGGGGGCCCATGGGTCCA
88 GCTTCTCCCCTGGGACCTGGTTTGCCGATGGGGCCCATCGGGCCAGGTAAG
89 CCCTTGGGACCCAAAGGACCAGTACTGCCATTAGTCCTTCGGGTCCAGTG
90 GGGCCCACTTCGCCTTTATCCCCCTTCTGCCCTGAGGGCAGTCTCTCCTGG
91 CAGCCCTTGCTCTCCTGTAGACCAATGGATCCCTTTGGGCCATGTTTCCCCG
92 GAGATCCTCTGGAGCCTGATCACCTTTGATGCCTTTTGCTTCAACTCTTCCA
93 TCTGCTCCTGTCTCCTTTCTCCCCACGAATCCATCCTTTCCTGACCACAGA
94 TGTCTGTTCTCCTGCGTC

95 **rAAV9-cTnT promoter-ctrp9-flag adeno-associated virus packaging**

96 The recombinant plasmid pAAV-cTnT promoter-Full Ctrp9-FLAG containing the gene
97 of interest was introduced into 293AAV cells, with plasmid pAAV-ZsGreen as control
98 virus. The titer of virus was 5×10^{12} vg/mL.

99

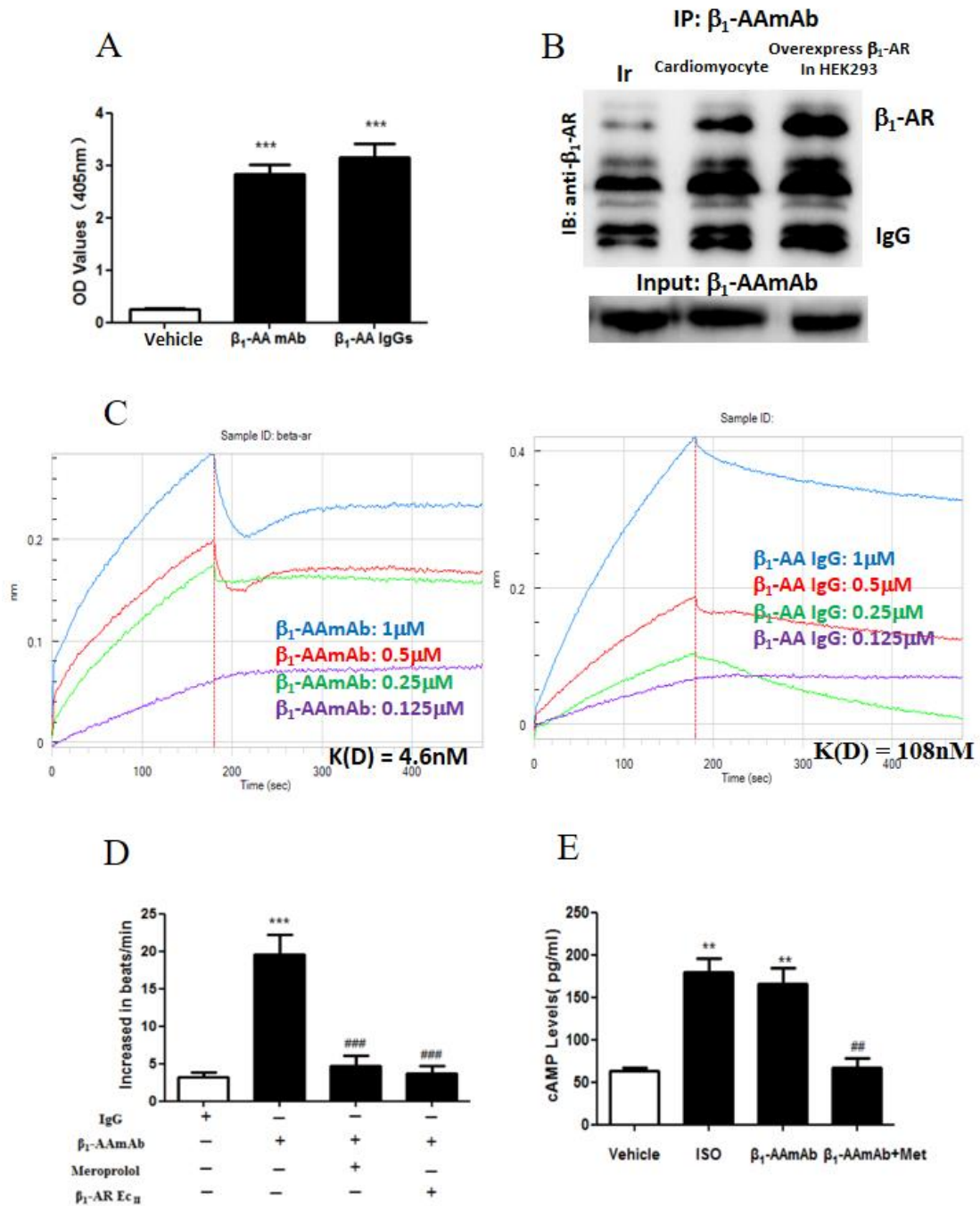
100

101

102

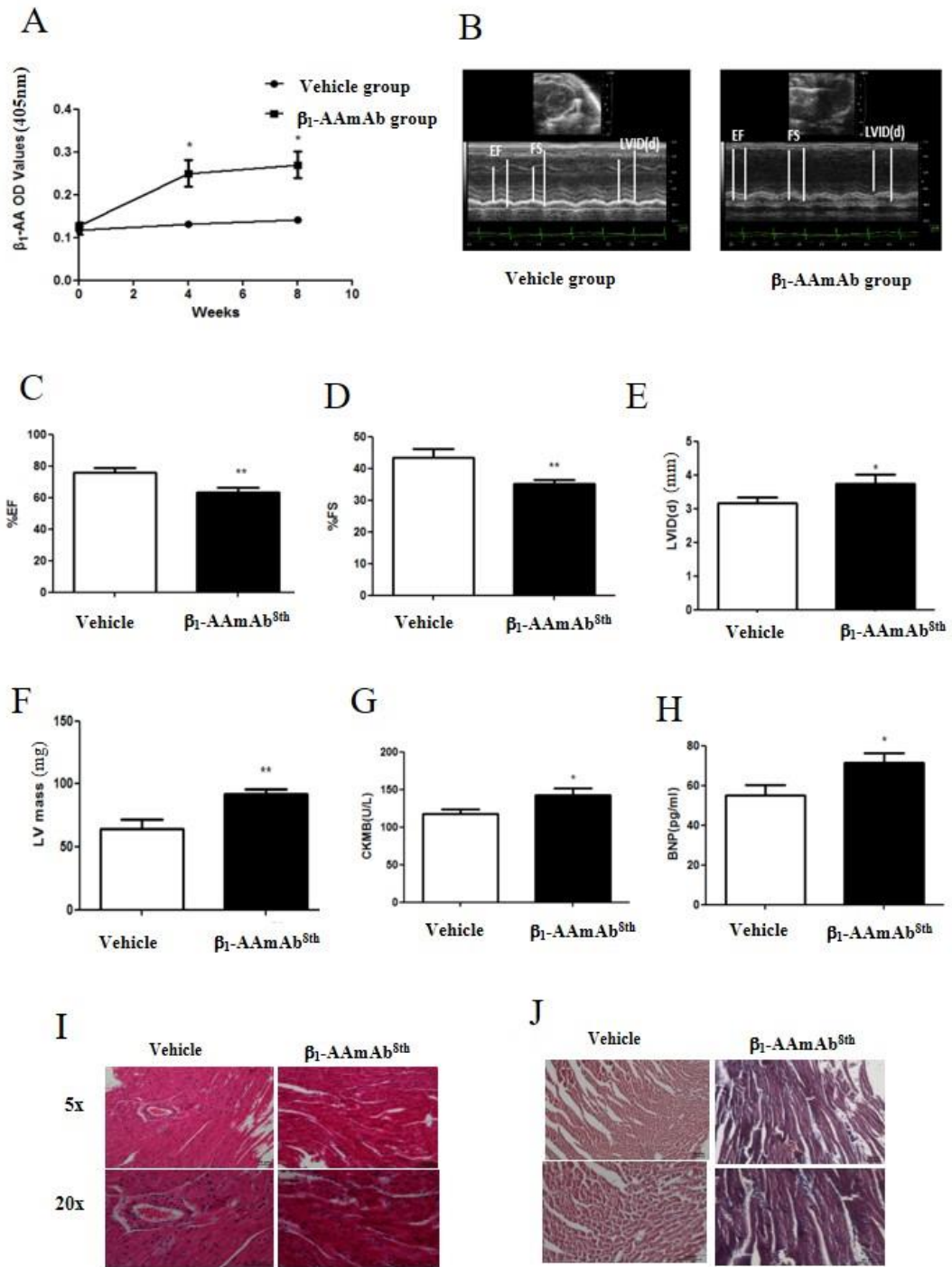
103

Supplementary Fig. 1



108 **mAb**). **(A)** β_1 -AAmAb levels in the supernatant of hybridoma cells were detected by
109 ELISA. **(B)** The binding of β_1 -AAmAb with β_1 -ARs on neonatal cardiomyocytes was
110 determined by Co-immunoprecipitation. **(C)** Bio-layer interferometry (BLI) technique
111 were performed to detect the binding and affinity of β_1 -AAmAb/ β_1 -AA IgG for β_1 -AR.
112 **(D)** The increased beating frequency of primary neonatal rat cardiomyocytes was
113 counted to evaluate the activity of β_1 -AAmAb, **(E)** The effect of β_1 -AAmAb (10^{-7} mol/l)
114 or isoproterenol (1 μ mol/l) on cAMP production (expressed as pg/ml) in rat neonatal
115 cardiomyocytes was examined by ELISA, , n=6, ISO: isoproterenol, MET: metoprolol.
116 Data presented as mean \pm SD. ***P <0.001 vs. vehicle or IgG, **P <0.01 vs. vehicle group,
117 ##P <0.01, ###P <0.001 vs. β_1 -AAmAb, n=6 per group.

Supplementary Fig. 2



118

119 **Fig S2. Long-term existence of β_1 -AAmAb induced ventricular remodeling. (A)**

120 The level of β_1 -AA at different time points during the treated 8 weeks. **(B)** Images are

121 representative of echocardiogram at the 8th week. **(C-F)** The LVEF %, FS%, LVID (d),

122 and LV mass of β_1 -AA positive group and vehicle group mice during the 8 weeks. **(G-**
123 **H)** The level of CKMB and BNP of β_1 -AA positive group and vehicle group mice
124 during the 8 weeks. **(I)** HE staining of the heart. **(J)** Masson's trichrome staining of
125 heart tissues. n=8, *P<0.05, **P<0.01 vs. vehicle. Vehicle group is saline group for 8w.
126 *EF*: Left ventricular ejection fraction; *FS*: percent fractional shortening; *LVID (d)*: left
127 ventricular diastolic diameter; *β_1 -AAmAb*: β_1 -AA monoclonal antibody; *CKMB*:
128 Creatine kinase isoenzyme MB; *BNP*: Brain natriuretic peptide.

129

130

131

132

133

134

135

136

137

138

139

140

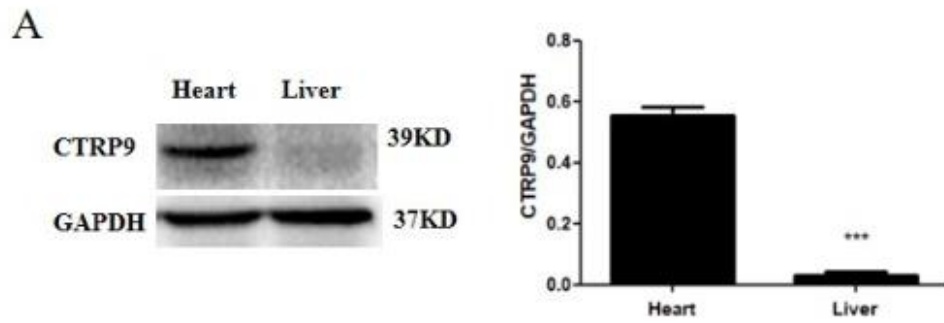
141

142

143

144

Supplementary Fig. 3



145

146 **Fig S3. The expression of CTRP9 in heart and liver. n=8, ***P<0.001 vs. heart.**

147

148

149

150

151

152

153

154

155

156

157

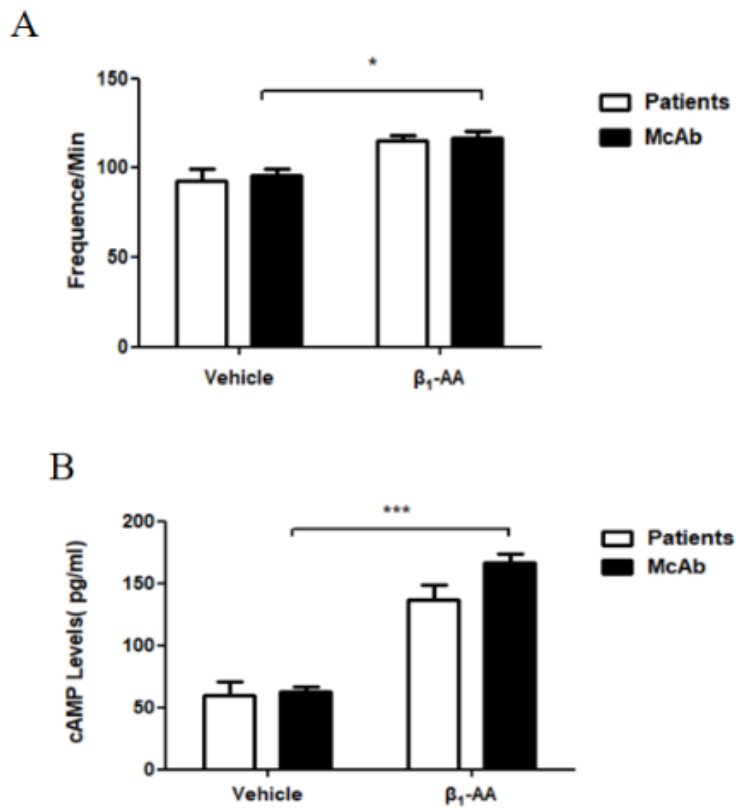
158

159

160

161

Supplementary Fig. 4



162

163 **Fig S4. Functional assays with β_1 -AA IgG purified from individual CAD patient**

164 (A) β_1 -AA IgG from β_1 -AA positive CAD patients increased the beat frequency of

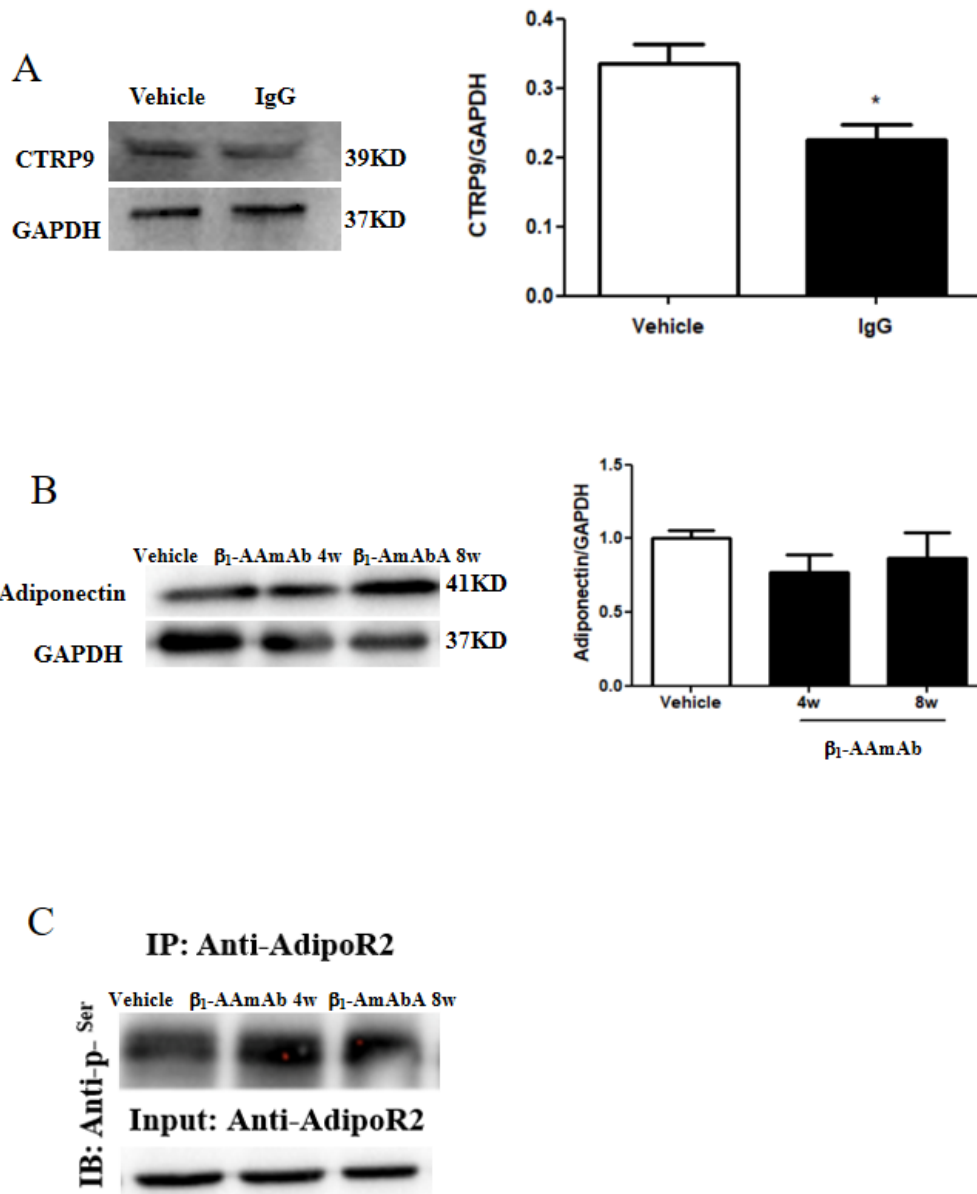
165 cultured cardiomyocytes. (B) The effect of β_1 -AA IgG on the production of cAMP

166 (expressed as pg/ml) in NRVMs by ELISA, * $P < 0.05$ *** $P < 0.001$ vs. vehicle. Data were

167 presented as mean \pm SD of 6 independent experiments. *IgG*: immunoglobulin fractions

168 G; *CAD*: Coronary heart disease;

Supplementary Fig. 5



169

170 **Fig S5.** (A) IgG from β_1 -AA-positive CAD patients decreased the expression of CTRP9

171 in neonatal rat cardiomyocytes, * $P < 0.05$ vs. vehicle, $n = 5$. (B) There is no change of

172 Adiponectin in cardiac tissue. $n = 8$ /group. (C) There is no change of AdipoR2 in cardiac

173 tissue. n=8/group. Vehicle group is saline group for 8w. *CAD*, Coronary heart disease;

174 *IgG*: immunoglobulin fractions G.

175